Perturbative resummed series for top quark production in hadron reactions

Edmond L. Berger and Harry Contopanagos

High Energy Physics Division, Argonne National Laboratory, Argonne, Illinois 60439

Our calculation of the total cross section for inclusive production of $t\bar{t}$ pairs in hadron collisions is presented. The principal ingredient of the calculation is resummation of the universal leading-logarithm effects of gluon radiation to all orders in the quantum chromodynamics coupling strength, restricted to the region of phase space that is demonstrably perturbative. We derive the perturbative regime of the resummed series, starting from the principal-value resummation approach, and we isolate the perturbative domain in both moment space and, upon inversion of the corresponding Mellin transform, in momentum space. We show that our perturbative result does not depend on the manner nonperturbative or infrared effects are handled in principal-value resummation. We treat both the quark-antiquark and gluon-gluon production channels consistently in the $\overline{\text{MS}}$ factorization scheme. We compare our method and results with other resummation methods that rely on the choice of infrared cutoffs. We derive the renormalization or factorization scale dependence of our resummed cross section, and we discuss factorization scheme dependence and remaining theoretical uncertainties, including estimates of possible nonperturbative contributions. We include the full content of the exact next-to-leading order calculation in obtaining our final results. We present predictions of the physical cross section as a function of top quark mass in proton-antiproton reactions at center-of-mass energies of 1.8 and 2.0 TeV. We also provide the differential cross section as a function of the parton-parton subenergy. [S0556-2821(96)01415-4]

I. INTRODUCTION

In hadron interactions at collider energies, the main production mechanisms for inclusive top-quark–top-antiquark ($t\bar{t}$) production, as modeled in perturbative quantum chromodynamics (PQCD), involve parton-parton collisions. The perturbative series begins at second order $O(\alpha_s^2)$ in the strong coupling strength α_s. At this order, the parton subprocesses are

$$i + j \rightarrow t + \bar{t}, \tag{1}$$

where the initial partons i, j are either a quark-antiquark ($q\bar{q}$) or a gluon pair (gg). In higher orders, gluons are radiated in these two production channels, and there are additional production channels, such as $qg \rightarrow t\bar{t}q$. The gluonic radiative corrections to the lowest-order channels create large enhancements of the partonic cross sections near the top pair production threshold [1,2]. The magnitude of the $O(\alpha_s^3)$ corrections implies that fixed-order perturbation theory will not necessarily provide reliable quantitative predictions for ($t\bar{t}$) pair production at Fermilab Tevatron energies. A resummation of the effects of gluon radiation to all orders in perturbation theory is called for in order to improve the reliability of the theory. This was the main motivation for the published resummation calculations of $t\bar{t}$ production [3–5].

In a prior paper, we presented a brief exposition of our method of resummation and its application to $t\bar{t}$ production [5]. Our guiding principle is the all-orders resummation of the universal leading-logarithm effects of initial-state radiation, restricted to the region of phase space which is manifestly *perturbative*. Our purpose in this paper is to expand upon our earlier theoretical and phenomenological discus-sion. We provide a detailed exposition of our approach, highlight the similarities and differences with Refs. [3,4], and show that our predictions are independent of the particular regularization of the infrared and nonperturbative regions imposed by principal-value resummation (PVR). We present predictions of the inclusive top-quark production cross section as a function of top-quark mass in proton-antiproton reactions at center-of-mass energies $\sqrt{S} = 1.8$ and 2.0 TeV, and in proton-proton reactions at the energies of the CERN Large Hadron Collider (LHC). We demonstrate that the renormalization or factorization scale dependence of our resummed cross sections is very modest. At the end, we speculate on modeling the unknown dynamics of the nonperturbative region and its possible contribution to the cross section.

In ''infrared safe'' processes, such as the total cross section for e^+e^- annihilation to hadrons, there is only one physical scale that characterizes the perturbative cross section, namely the total energy of the electroweak initial state. In hadron-hadron scattering, according to the factorization theorem of PQCD, the cross sections for the partonic subprocesses are the main object of theoretical calculations. In most hard-scattering processes, however, partonic cross sections are not free of singularities. Initial-state hadronic interactions require that a nontrivial ''mass factorization'' be performed in order to absorb a singular part of these cross sections into a redefinition of the long-distance parton distribution functions in a universal, process-independent way. Once mass factorization is performed, the object of theoretical interest is the short-distance part of the partonic cross sections (the ''hard part''). The hard part usually depends on more than one momentum scale, typically because of gluon radiation. The hard part is calculated as a series in the strong coupling strength of PQCD, and the domain of applicability of the series is a function of *all* pertinent momentum scales. In

determining the region of applicability of this series, one encounters difficulties including, but not limited to, infrared renormalons [6]. Most discussions (not necessarily in agreement) on the range of validity of PQCD have focused on momentum-scaling properties of Green's functions [7,8], but color factor constants are an equally important aspect of the series and should be taken seriously into account. Both can contribute to the breakdown of PQCD. Although the former have a more ''dynamical'' appearance because they depend on momentum, both create difficulties that are combinatoric in nature. Infrared renormalons create factorial growth associated with massless vacuum polarization diagrams, and large constants enhance the strength of the partonic interactions according to their corresponding fields in color space. Among the many virtues of Ref. [3] is the demonstration that large multiplicative color factors are indeed extremely important in realistic situations. Their effects transcend standard operator-product-expansion (OPE) arguments to the effect that nonperturbative effects are suppressed by at least Λ^2/m^2 or approaches that are usually formal and model dependent [8]. We treat this problem in detail in the present paper from the realistic viewpoint of applying resummation to a specific reaction of significant phenomenological importance. From an operator point of view, however, this is an issue that deserves further investigation, to be addressed in a future publication [9].

Top-quark production, Eq. (1), embodies all the issues mentioned above. An instructive illustration can be found in the $O(\alpha_s^3)$ calculation of the partonic hard part, or loosely speaking, the ''partonic cross section'' for heavy flavor production [1]. Figures 12 and 13 of the first paper in Ref. [1] show that the $O(\alpha_s^3)$ hard part is much larger than the leading-order $O(\alpha_s^2)$ hard part *in specific regions of partonic subenergy*. Analogous results are shown here in Fig. 7, to be discussed in Sec. V. Not all of the range of the partonic subenergy can be considered part of the perturbative domain *despite the fact* that, at finite orders, the resulting radiative corrections are integrable throughout that phase space and yield finite inclusive predictions. Dominance of the higher-order contributions in the $q\bar{q}$ and gg channels near threshold, and in the gg channel at large values of the subenergy, feeds back (albeit not as enhanced) to the physical cross sections obtained after convolution with parton densities. In this paper, we limit our attention to processes in which the near-threshold region is the most important influence. At Fermilab Tevatron collider energies, the next-to-leading-order enhancement of the top-quark cross section is approximately 25% relative to the leading-order value. For comparison, at a scale specified by the mass m of the top quark, $\alpha_s(m) \simeq 10\%$. Top-quark production at the Tevatron is one that involves *multiple* QCD scales.

Dominance of the next-to-leading-order contributions to top-quark production near threshold in the $q\bar{q}$ and gg channels is mentioned earlier in this Introduction as a primary motivation for theoretical study of resummation of the effects of gluon radiation to all orders. One method of resummation was implemented for $t\bar{t}$ pair production some time ago [3,4]. In most resummation methods, the threshold corrections are exponentiated into a function of the QCD running coupling strength, α_s, evaluated at a variable momentum scale which is a measure of the radiated momentum. To recover the inclusive cross section, one then integrates over the available radiation phase space down to the partonic threshold. An inherent ambiguity and limitation of the method of Ref. [3] is the introduction of undetermined infrared (IR) cutoffs. The need for these cutoffs arises because the kinematically allowed region meets the Landau pole of the QCD running coupling. More generally, the exponentiation of logarithmic corrections results in essential singularities, whether expressible as singularities of the running coupling or not, while a finite-order expansion in terms of α_s at a fixed hard scale exhibits a polynomial (and hence integrable) dependence on the logarithms. Since the IR cutoff dependence is exponentiated in Ref. [3], the sensitivity of their predicted cross sections to the value of the cutoffs is very significant numerically, especially when multiplicative color factors are large, as in the gg production channel.

An advantage of our resummation approach [5] is that it does not require arbitrary IR cutoffs. We use the principal-value resummation (PVR) technique [10] to bypass the Landau poles and associated renormalon singularities, and we obtain a mathematically unambiguous expression for the resummation exponent in moment space. The PVR procedure allows us to identify the *perturbative* properties of the resummation exponent and to separate these from the *nonperturbative* behavior of the exponent. The perturbative properties are obtained through a short-distance asymptotic approximation valid in a specific region of moment space. The separation is in turn used to derive a perturbative regime for the hard part itself in moment space, which is more restricted due to large color factors and exponentiation. The inversion of the Mellin transform [11] provides the hard part directly in momentum space, and we obtain a resummed perturbative expression for the partonic cross section, along with the corresponding determination of the perturbative regime in momentum space. This new method should be contrasted with the resummation approach of Ref. [3] where explicit use of IR cutoffs makes a perturbative separation impossible.

It may be argued that adoption of the PVR technique is the adoption of a model and that the IR cutoff dependence of Ref. [3] is merely concealed. We argue that this is not the case precisely because we apply our method only in a well-defined perturbative region. To the extent that PVR is a model, it is a model only for the nonperturbative region that we do not include. The main physical issue on which we focus is not the finiteness PVR regularization imposes. Rather, it is how this finiteness *helps us to probe* the asymptotic properties of the perturbative cross section. Therein lies part of the usefulness of PVR, even though it is possible that the regularization it imposes throughout phase space, including the nonperturbative regime, may be physically significant. For example, PVR applied to the Drell-Yan process at fixed target energies is in excellent agreement with experiment [12]. We will discard the cross section in the nonperturbative region as model dependent, notwithstanding its finiteness in PVR.

The perturbative regime should be independent of infrared regulators, including the principal-value regulator. To demonstrate this independence, we show in detail in this paper how one may obtain the same expressions as ours for the perturbative resummed cross section, independently of any

regularization. To do so, we must make two physically plausible assertions about the perturbative behavior of the resummation exponent in moment space, assertions that are natural ingredients of the PVR exponent.

Our resummation includes the *leading* large threshold logarithmic contributions to all orders in perturbation theory. These contributions are interpreted to be universal, characteristic of the initial states that produce the hard scattering. They are common with other hard-scattering processes, notably massive lepton-pair ($l\bar{l}$) production, the Drell-Yan process. A complete $O(\alpha_s^2)$ calculation is available for the Drell-Yan process, meaning that the logarithmic structure is known explicitly in that case to one order in perturbation theory higher than for $t\bar{t}$ production. Final-state effects, which differentiate among hard-scattering processes, produce subleading logarithmic structures that are not universal and should not be included in a universal resummation approach. It is possible, and even probable, that resummation of subleading large logarithms from final-state and interference effects can be accomplished, but such a resummation will be process dependent. For the application we have in mind, its numerical effects will be subleading in nature. We consider the resummation of final-state logarithms beyond the scope of this work.

An outline of this paper is as follows. In Sec. II we present the kinematics of the inclusive cross section for top-quark production and the form of its resummed version. We include a general discussion on counting powers of logarithms for the hard part at finite orders and for its resummed version. In Sec. III we present the perturbative properties of the PVR resummation exponent E in moment space, in both the modified minimal subtraction ($\overline{\text{MS}}$) and deep-inelastic-scattering (DIS) factorization schemes, as well as its renormalization-group (RG) invariance properties. We consider a formally identical exponent but without regularization, and we examine its factorial growth in moment space in order to compare the resulting perturbative asymptotic approximation *at fixed moments* with the one resulting from PVR. The two perturbative approximations are in agreement with each other, but the one without the PVR prescription does not directly constrain the moment variable since it derives from an unregularized expression that exists only formally. We offer additional physically motivated criteria one could use in this latter approach to constrain the moment variable, and we show that the resulting constraints are similar to those imposed by PVR. Using a heuristic argument, we describe how one may estimate the perturbative regime for the exponentiated hard part itself in moment space.

In Sec. IV we discuss the universality of the threshold logarithmic corrections in comparison with massive lepton-pair ($l\bar{l}$) production, using threshold asymptotics and the results of the complete $O(\alpha_s^2)$ calculation of heavy quark production [1,2]. We examine the detailed structure of the hard-scattering function in the gluon radiation phase space (momentum space) and the corresponding determination of the perturbative regime in that space. The hard-scattering function is proportional to $\exp(E)$, which resums the threshold corrections directly. The inversion of the Mellin transform produces a hard part in momentum space that includes a series of subleading structures deriving from E [11]. It is

this latter expression that is best suited for the determination of the perturbative regime in momentum space. The two determinations of the perturbative regime for the cross section in moment and momentum space are in good agreement with each other. We conclude that the resummed perturbative partonic cross section derived from the PVR approach is independent of the PVR regularization and is valid in a well-established perturbative regime. It is derived basically from simultaneous minimization of the factorial growth of IR renormalons *and* color factor combinatorics in the exponentiated hard part.

In Sec. V we discuss the numerical properties and phenomenological behavior of the resummed partonic and physical cross sections, for both the $q\bar{q}$ and gg production channels, in the $\overline{\text{MS}}$ and DIS factorization schemes. Predictions are presented in the form of both figures and tables of the inclusive cross section for top-quark production as a function of top mass in proton-antiproton collisions at $\sqrt{S}=1.8$ and 2.0 TeV. We display the factorization-renormalization scale dependence of the physical cross sections and provide extensive comparisons with the corresponding quantities of Ref. [3]. We address the issue of perturbative theoretical uncertainties in both our approach and that of Refs. [3,4]. In Sec. VI we present estimates of nonperturbative uncertainties based on physically motivated assumptions about the behavior of the cross section in that regime. We summarize our conclusions in Sec. VII.

II. PRODUCTION KINEMATICS AND RESUMMATION

In this section we begin with expressions for the partonic and physical cross sections in finite orders of QCD perturbation theory and the associated kinematics of $t\bar{t}$ production. Subsequently, we present a resummed expression for the partonic cross section in PVR, based on universality of the leading threshold corrections with those in massive lepton-pair ($l\bar{l}$) production. In this paper, we use uppercase S to denote the square of the total energy in the hadron-hadron system and lowercase s for the square of the energy in the partonic system.

A. Next-to-leading-order cross section and kinematics

We start with the next-to-leading-order one-particle inclusive partonic differential cross section in the DIS factorization scheme. We use the notation $\alpha(\mu) \equiv \alpha_s(\mu)/\pi$, where μ is the common renormalization-factorization hard scale of the problem. A perturbative quantity R is expanded as $R^{[i]} = \sum_{j=0}^{i} \alpha^j R^{(j)}$, where $R^{(j)}$ is the order α^j radiative correction to R, *above the leading order*. Unless otherwise specified, $\alpha \equiv \alpha(\mu = m)$ where m is the mass of the top quark. Following the notation of Ref. [3] for the subprocess

$$i(k_1) + j(k_2) \rightarrow t(p_1) + \bar{t}(p_2) + g(k), \qquad (2)$$

and defining the partonic invariants

$$s = (k_1 + k_2)^2, \quad t_1 = (k_2 - p_2)^2 - m^2,$$

$$u_1 = (k_1 - p_2)^2 - m^2, \quad s_4 = s + t_1 + u_1, \qquad (3)$$

we express the partonic differential cross section as

$$m^2 s^2 \frac{d^2\sigma_{ij}^{(1)}}{dt_1 du_1}(s,t_1,u_1) = 2C_{ij}\bar{D}_1(s_4;\Delta)\sigma_{ij}^B(s,t_1,u_1) + R. \tag{4}$$

In Eq. (4), $\sigma_{ij}^B(s,t_1,u_1)$ is the lowest-order Born cross section, expressed in terms of three-particle final-state variables, and the remainder R stands for terms that do not contain leading logarithmic corrections near threshold. The quantity C_{ij} is the color factor for the ij production channel, and

$$\bar{D}_1(s_4,m^2;\Delta) \equiv \frac{m^2}{s_4}\ln\left(\frac{s_4}{m^2}\right)\Theta(s_4-\Delta) + m^2\delta(s_4)\frac{1}{2}\ln^2\left(\frac{\Delta}{m^2}\right), \tag{5}$$

where Δ is understood in the distribution sense:

$$\lim_{\Delta\to 0}\int_0^y d(s_4/m^2)\phi(s_4/m^2)\bar{D}_1(s_4,m^2;\Delta). \tag{6}$$

In Eq. (3), s_4 is a measure of the inelasticity of the radiative process, and it is proportional to the gluon momentum k. One can show that $s_4 = 2k\cdot p_1$ and hence, for soft gluons, $s_4\to 0$. The distribution $\bar{D}_1$ can be shown to be a ''plus'' distribution. Indeed, define $s_4/m^2 \equiv 1-z$ and

$$D_1(z) \equiv \left(\frac{\ln(1-z)}{1-z}\right)_+. \tag{7}$$

Then, for any smooth function ϕ,

$$\int_{1-y}^1 dz\,\phi(1-z)D_1(z) \equiv \int_{1-y}^1 dz[\phi(1-z)-\phi(0)]\frac{\ln(1-z)}{1-z}$$
$$-\phi(0)\int_0^{1-y} dz\frac{\ln(1-z)}{1-z}. \tag{8}$$

The right-hand side can be written as

$$\int_{1-y}^{1-\epsilon} dz\,\phi(1-z)\frac{\ln(1-z)}{1-z} - \phi(0)\int_{1-y}^{1-\epsilon} dz\frac{\ln(1-z)}{1-z} + \sum_{k=1}^\infty \frac{\phi^{(k)}(0)}{k!}\int_{1-\epsilon}^1 dz(1-z)^{k-1}\ln(1-z) - \phi(0)\int_0^{1-y} dz\frac{\ln(1-z)}{1-z}. \tag{9}$$

The series tends to zero as $\epsilon\to 0$, and the result is

$$\int_{1-y}^1 dz\,\phi(1-z)D_1(z) = \int_{1-y}^{1-\epsilon} dz\,\phi(1-z)\frac{\ln(1-z)}{1-z} + \phi(0)\frac{1}{2}\ln^2\epsilon = \int_\epsilon^y \frac{ds_4}{s_4}\phi(s_4/m^2)\ln\left(\frac{s_4}{m^2}\right) + \phi(0)\frac{1}{2}\ln^2\epsilon. \tag{10}$$

This is the result obtained also from Eqs. (5) and (6) with the identification $\epsilon \equiv \Delta/m^2$. Hence we have proved the identity $\bar{D}_1(s_4,m^2;\Delta) = D_1(z)$, with $s_4/m^2 \equiv 1-z$. The identification $s_4/m^2 = 1-z$ is suggestive of the similarity of the present reaction, $t\bar{t}$ production, with the Drell-Yan process [10,12] where $z = Q^2/s$ is the fraction of the squared invariant energy carried by the dilepton pair. The threshold is at $z\to 1$, as it is in our case as well. We use z rather than s_4 in this paper to stress the similarity between these two reactions.

We can write the differential cross section, including the Born term, as

$$m^2 s^2 \frac{d^2\sigma_{ij}^{[1]}}{dt_1 du_1}(s,t_1,u_1) = \left\{ \delta(1-z) + \alpha 2C_{ij}\left(\frac{\ln(1-z)}{1-z}\right)_+ \right\}\sigma_{ij}^B(s,t_1,u_1). \tag{11}$$

If we compare the above expression and the corresponding one for the Drell-Yan process, we may verify that the logarithmic structure is identical through next-to-leading order. It is important to note here that the exact calculation of the cross section for $t\bar{t}$ production, including the remainder term R in Eq. (4), contains subleading terms, such as $[1/(1-z)]_+$, as well as constants. These structures are not common to the Drell-Yan reaction, and they cannot be resummed as part of initial-state radiation only. As in Ref. [3], we disregard these subleading structures in our resummation. We demonstrate the nonuniversal character of these subleading corrections in Sec. IV.

Following Ref. [3] we integrate Eq. (11) over the whole partonic phase space. Using the appropriate kinematic bounds, we obtain

$$\sigma_{ij}^{[1]}(\eta,m^2) = \int_{1-4(1+\eta)+4\sqrt{1+\eta}}^1 dz\left\{ \delta(1-z) + \alpha 2C_{ij}\left(\frac{\ln(1-z)}{1-z}\right)_+ \right\}\bar{\sigma}_{ij}^B(\eta,z,m^2), \tag{12}$$

where

$$\bar{\sigma}_{ij}^B(\eta,z,m^2) \equiv \frac{\sqrt{(s/m^2-1+z)^2-4s/m^2}}{2s^2}\int_{-1}^1 d\cos\theta\,\sigma_{ij}^B(s,t_1,u_1). \tag{13}$$

The kinematic transformations

$$t_1 = -\frac{1}{2}m^2[s/m^2 - 1 + z - \sqrt{(s/m^2 - 1 + z)^2 - 4s/m^2}\cos\theta],$$

$$u_1 = -\frac{1}{2}m^2[s/m^2 - 1 + z + \sqrt{(s/m^2 - 1 + z)^2 - 4s/m^2}\cos\theta],$$

$$s = 4m^2(1 + \eta) \tag{14}$$

are used to obtain Eqs. (12) and (13). The lower limit of integration in Eq. (12) is derived from the kinematics of Eqs. (2) and (3), namely $s_4 \leq s - 2m\sqrt{s}$.

As in the Drell-Yan case, one may eliminate the δ function and plus distribution in Eq. (12) by integrating by parts. Using the identity

$$\int_z^1 dx[f(x)]_+ = -\int_0^z dx f(x), \tag{15}$$

and the kinematic constraint

$$\bar{\sigma}_{ij}^B(\eta, z = 1 - 4(1 + \eta) + 4\sqrt{1 + \eta}), m^2) = 0, \tag{16}$$

we arrive at the following expressions for the cross sections. In the DIS factorization scheme,

$$\sigma_{ij}^{[1]}(\eta, m^2) = \int_{1 - 4(1 + \eta) + 4\sqrt{1 + \eta}}^1 dz\{1 + \alpha C_{ij}\ln^2(1 - z)\}\sigma_{ij}'(\eta, z, m^2), \tag{17}$$

and, in the $\overline{\text{MS}}$ scheme,

$$\sigma_{ij}^{[1]}(\eta, m^2) = \int_{1 - 4(1 + \eta) + 4\sqrt{1 + \eta}}^1 dz\{1 + \alpha 2C_{ij}\ln^2(1 - z)\}\sigma_{ij}'(\eta, z, m^2), \tag{18}$$

$$\sigma_{ij}'(\eta, z, m^2) \equiv \frac{d}{dz}\bar{\sigma}_{ij}^B(\eta, z, m^2). \tag{19}$$

The explicit expression for the derivative of the Born cross section in the $q\bar{q}$ channel is

$$\sigma_{q\bar{q}}'(\eta, z, m^2) = \frac{2}{3}C_F\pi^3\alpha^2\frac{\tau}{s}x(z)\left\{\sqrt{x^2(z) - 4\tau} + \frac{2\tau}{\sqrt{x^2(z) - 4\tau}}\right\}, \tag{20}$$

where

$$x(z) \equiv 1 - (1 - z)\tau, \tag{21}$$

$\tau \equiv m^2/s = [4(1 + \eta)]^{-1}$, and $C_F = 4/3$. In the gg channel,

$$\sigma_{gg}'(\eta, z, m^2) = \frac{3}{16}\pi^3\alpha^2 C_F\frac{\tau}{s}\left[C_F\left\{-\left(1 - \frac{4\tau}{x^2(z)}\right)^{3/2} + \left(1 - \frac{4\tau}{x^2(z)} + \frac{24\tau^2}{x^4(z)}\right)\ln y(z) + \left(2 + \frac{4\tau}{x^2(z)} - \frac{32\tau^2}{x^4(z)}\right)\frac{1}{\sqrt{1 - \frac{4\tau}{x^2(z)}}}\right\}\right.$$

$$\left. + C_A\left\{-\left(x^2(z) + \frac{52}{3}\right)\sqrt{1 - \frac{4\tau}{x^2(z)}} - \frac{4\tau^2}{x^2(z)}\ln y(z) - \left(\frac{4\tau}{3} - \frac{4\tau^2}{3x^2(z)}\right)\frac{1}{\sqrt{1 - \frac{4\tau}{x^2(z)}}}\right\}\right], \tag{22}$$

where $C_A = 3$ and

$$y(z) \equiv \frac{1 + \sqrt{1 - [4\tau/x^2(z)]}}{1 - \sqrt{1 - [4\tau/x^2(z)]}}. \tag{23}$$

B. Resummation and power counting

The large logarithms near threshold, both at finite orders and in resummation, play a major role in our considerations. In this section, we provide a general description that establishes the notion of leading and subleading logarithmic structures and the way we use this terminology. Generalizing the

notation of Eqs. (17) and (18), we write the partonic cross section resulting from a finite-order perturbative calculation as

$$\sigma^{[k]}(\eta, m^2) = \int_{1-4(1+\eta)+4\sqrt{1+\eta}}^{1} dz H^{[k]}(z,\alpha)\sigma'_{ij}(\eta,z,m^2).$$

(24)

Here

$$H^{[k]}(z,\alpha) = \sum_{m=0}^{k} \alpha^m \sum_{l=0}^{2m} c(l,m)x_z^l,$$

$$\text{with } x_z \equiv \ln\left(\frac{1}{1-z}\right),$$

(25)

and $c(l,m)$ are calculable numerical coefficients. In this representation, the classification of the logarithmic structures is obvious. Leading logarithms are the monomials proportional to $c(2m,m)$, first subleading logarithms the monomials proportional to $c(2m-1,m)$, etc. Since we are concerned with threshold enhancements, $z\to1$ or, equivalently, $x_z\to+\infty$, the nomenclature is related directly to the numerical importance of the corresponding logarithmic structures in the cross section.

At finite orders, the logarithmic structures are integrable near threshold, and their contributions to the cross section are finite, provided the Born cross sections are also integrable (as is indeed the case). For purposes of demonstration, let us assume that the Born cross section behaves as $(1-z)^\nu$, $-1<\nu$. Using

$$x_z^l = \ln^l\left(\frac{1}{1-z}\right) = (-1)^l \lim_{\epsilon\to0}\left(\frac{\partial}{\partial\epsilon}\right)^l (1-z)^\epsilon,$$

(26)

and denoting $L(\eta) \equiv 1-4(1+\eta)+4\sqrt{1+\eta}$, we find

$$H^{(l,m)}(\eta,\alpha) \equiv \alpha^m c(l,m) \int_{L(\eta)}^{1} dz(1-z)^\nu x_z^l$$

$$= \alpha^m c(l,m)(-1)^l \lim_{\epsilon\to0}\left(\frac{\partial}{\partial\epsilon}\right)^l \int_{L(\eta)}^{1} dz(1-z)^{\nu+\epsilon}$$

$$= \alpha^m c(l,m)(-1)^l \lim_{\epsilon\to0}\left(\frac{\partial}{\partial\epsilon}\right)^l \left(\frac{L(\eta)^{1+\nu+\epsilon}}{1+\nu+\epsilon}\right)$$

$$= H_0(\eta)K^{(l,m)}(\eta,\alpha),$$

(27)

where

$$H_0(\eta) = \frac{1}{\nu+1}[1-L(\eta)]^{\nu+1}$$

(28)

is the ''Born'' cross section, and

$$K^{(l,m)}(\eta,\alpha) = \alpha^m c(l,m)\frac{l!}{(1+\nu)^l}$$

$$\times \sum_{j=0}^{l} (-1)^j(1+\nu)^j\ln^j[1-L(\eta)]$$

(29)

is the ''K factor'' due to the $c(l,m)$ radiative correction in Eq. (25). Near threshold,

$$\lim_{\eta\to0} L(\eta) \simeq 1-2\eta.$$

(30)

While both $H_0(\eta)$ and $H^{(l,m)}(\eta,\alpha)$ vanish as $\eta\to0$, the function $K^{(l,m)}(\eta,\alpha)$ diverges as the lth power of the logarithm. Relative to the lowest-order term, its contribution can be arbitrarily large in η space for a sufficiently high power l, despite the perturbative suppression α^m. The logarithmic terms will have a significant effect on the physical cross section, obtained as the integral over η of Eq. (27) convoluted with the parton distributions, especially if the hadronic center-of-mass energy is such that the support of this integration emphasizes the threshold region. Under such circumstances we may view η as a second important physical parameter, in addition to m, that is probed phenomenologically. The two-scale nature of the problem is evident in that we have one hard scale m and a ratio $\eta=(s/4m^2)-1$ whose important physical domain is near 0. The perturbative QCD series is required to have reliable behavior in *both* variables, m and η.

The objective of resummation is to derive formulas, based on the properties of QCD as a field theory, that provide a summation of the various classes of monomials in Eq. (25). In typical resummation methods, the partial sums of the hard part, Eq. (25), are replaced with a resummed hard function that contains the numerically important pieces of the partial sums, to all orders in PQCD. Most resummations of threshold effects result in exponentiation of the large logarithmic contributions. A generic resummation may result in an expression such as

$$\mathcal{H}(z,\alpha) \simeq e^{E(x_z,\alpha)}.$$

(31)

The principal content of resummation resides in the exponent $E(x_z,\alpha)$, which is typically a function of the QCD running coupling strength, integrated through intermediate momentum scales. The particular form of this function is fairly process independent and follows from general field-theoretical arguments [13]. For the present, we concentrate on power counting, ignoring complications specific to particular resummation methods. A large part of the remainder of the paper is devoted to the complications.

Under specific conditions that we analyze in detail later, the resummation exponent can be cast into a perturbative form similar to that of Eq. (25):

$$E(x_z,\alpha) = \sum_{m=1}^{N} \alpha^m \sum_{l=0}^{m+1} e(l,m)x_z^l.$$

(32)

The precise power structure above follows from first principles. For a resummation method to be realistic in practice, the exponent $E(x_z,\alpha)$ should be calculable in a finite number of steps. One consequence is that the exponent is not calculable with arbitrary precision, implying, in turn, a level of uncertainty in some of the coefficients $e(l,m)$, for specific ranges of l,m. The only consistent treatment of this limitation is to calculate the exponent in enough detail that the uncalculable coefficients in Eq. (32) accompany logarithmic structures x_z^l that are numerically insignificant in the range

where the representation Eq. (32) makes sense in the first place. As demonstrated explicitly in the Drell-Yan process [11], and as will become apparent below, use of the two-loop QCD running coupling strength is necessary in the calculation. Roughly speaking, the representation Eq. (32) is valid when $\alpha x_z < 1$. This inequality determines the limit of calculational accuracy of the exponent. The upshot is that the coefficients $e(l,m)$, $l \in \{0, m-1\}$, $m \geq 3$ are undetermined.

Because the exponent is the central object in resummation, most of the approximations are effected on that quantity. By way of definition we say that we resum *leading logarithms* when all $\{e(m+1,m)\}$ are determined, and *nonleading logarithms* when all $\{e(m,m)\}$ are determined in addition. Resummation of leading and nonleading logarithms has been done in detail for the Drell-Yan process [12]. It is important to note, however, that our definition is not identical to the obvious definition that exists at finite orders. The latter is contained in the former. In the next few paragraphs, we establish the relationship between the power counting of logarithms in resummation and the obvious finite-order definition at the beginning of this section.

Leading-logarithm resummation includes *all* leading logarithms at finite orders. Indeed, suppose we have performed leading-logarithm resummation. Then

$$E(x_z, \alpha) \simeq \sum_{m=1}^{N} \alpha^m e(m+1,m) x_z^{m+1}, \qquad (33)$$

and the kernel of the hard part is

$$\mathcal{H}(z, \alpha) = \prod_{m=1}^{N} e^{\alpha^m e(m+1,m) x_z^{m+1}}. \qquad (34)$$

To compare with finite-order PQCD, we must make a Taylor expansion of Eq. (34) in α. It is clear that all leading-logarithm coefficients in Eq. (25), $c(2m,m)$, are obtained from the set $\{e(m+1,m)\}$ of Eq. (34) and, more specifically, from $e(2,1)$ itself. Consider for example the Taylor expansion of the two first terms of the product of Eq. (34):

$$\sum_{k_1=0}^{\infty} \frac{\alpha^{k_1} x_z^{2k_1} e^{k_1}(2,1)}{k_1!} \sum_{k_2=0}^{\infty} \frac{\alpha^{2k_2} x_z^{3k_2} e^{k_2}(3,2)}{k_2!}. \qquad (35)$$

The general monomial of this product is

$$\frac{\alpha^{k_1+2k_2} x_z^{2k_1+3k_2} e^{k_1}(2,1) e^{k_2}(3,2)}{k_1! k_2!}, \qquad (36)$$

and the only terms that fit the set described by $c(2m,m)$ are $k_1 \in \mathbf{N}$, $k_2 = 0$. Therefore, $c(2m,m) = e^m(2,1)/m!$, and leading-logarithm resummation includes all finite-order leading logarithms, along with a specification of the values of these terms beyond the order in perturbation theory at which they may have been computed explicitly. It should be remarked that it includes *more*. The product of Eq. (34) generates upon expansion subleading logarithms in finite-order PQCD. For example, $k_1 \in \mathbf{N}$, $k_2 = 1$ in Eq. (36) are of the first-subleading kind $c(2m-1,m)$ of Eq. (25). These are not a closed set, i.e., they account only partially for all the subleading logarithms resulting from a finite-order calculation.

For example, to account for all $\{c(2m-1,m)\}$, a nonleading exponent in Eq. (32) would have to be calculated, i.e., all coefficients $\{e(m,m)\}$ in Eq. (32) would in addition have to be specified. Upon expansion, such a resummation of finite-order first subleading logarithms would produce a series

$$\mathcal{H}(z, \alpha) = \sum_{m=0}^{\infty} \alpha^m \sum_{l=m}^{2m} h(l,m) x_z^l, \qquad (37)$$

where each coefficient $h(l,m)$ is a product of $\{e(l,m)\}$'s.

We remark that Eq. (37) does not determine uniquely all finite-order coefficients $\{c(l \geq m,m)\}$, *for all values of m*, but it leaves a subset undetermined. To illustrate this point, consider the leading uncertainty in the resummation exponent. Since the one-loop running coupling constant produces all $\{e(m+1,m)\}$ and part of $\{e(m,m)\}$, $m \in \mathbf{N}$, and the two-loop running coupling constant produces the remaining pieces of $\{e(m \geq 2,m)\}$, the leading uncertainty in the exponent is $\delta \alpha^3 x_z^2$ in realistic resummations. This is the lowest order in α, highest order in x_z undetermined monomial that comes from expanding the three-loop running coupling strength in the exponent.

A product of the form

$$\sum_{k_1=0}^{\infty} \frac{\alpha^{k_1} x_z^{2k_1} e^{k_1}(2,1)}{k_1!} \sum_{k_2=0}^{\infty} \frac{\alpha^{3k_2} x_z^{2k_2} \delta^{k_2}}{k_2!} \qquad (38)$$

would then be present in the resummed hard kernel. The general monomial is

$$\frac{\alpha^{k_1+3k_2} x_z^{2(k_1+k_2)} e^{k_1}(2,1) \delta^{k_2}}{k_1! k_2!}. \qquad (39)$$

We wish to investigate the degree to which the second series in Eq. (38) maximally changes the coefficients $\{h(l,m)\}$ of Eq. (37). Setting $2(k_1+k_2) = 2(k_1+3k_2) - n$, we see that we obtain $k_2 = n/4$. Hence the minimum $n = 4$, and the minimum $k_2 = 1$. Maximum uncertainty arises in the coefficients

$$h(2m-4,m). \qquad (40)$$

The coefficients $\{h(l \geq m,m)\}$ are affected *for high enough m*. For example at minimum power of α, $m = 4$, the "diagonal" coefficient $h(4,4)$ is affected, at $m = 5$ the coefficients $h(6,5), h(5,5)$ are affected, etc. However, the leading, first-, second-, and third-subleading logarithms, as defined in finite-order power counting, are unaffected for any orders. These finite-order logarithmic structures are then resummed to all orders, by a resummation of leading and nonleading logarithms. It is unlikely that the affected structures are significant numerically in such a resummation, once we restrict ourselves to the perturbative regime in x_z.

We complete this section by returning to the reaction of interest, $t\bar{t}$ production. At this point, we invoke universality with the Drell-Yan case. Because the finite-order leading logarithms are identical in the $t\bar{t}$ and $l\bar{l}$ cases, we can resum them in $t\bar{t}$ production with the same function we use in the Drell-Yan case. According to Ref. [11], the structure of the kernel of the resummed hard part in the Drell-Yan case is

$$I(z,\alpha) = \delta(1-z) - \left(\frac{e^{E(x_z,\alpha)}}{1-z} \sum_{j=0}^{\infty} Q_j(x_z,\alpha) \right)_+ . \quad (41)$$

For simplicity, we drop the channel indices ij; $x_z \equiv \ln[1/(1-z)]$. We defer to Secs. III and IV an explanation of the various functions in this equation. One can therefore write the resummed partonic cross section as

$$\sigma_{ij}(\eta,m^2) = \int_{1-4(1+\eta)+4\sqrt{1+\eta}}^{1} dz I(z,\alpha) \sigma_{ij}^B(\eta,z,m^2). \quad (42)$$

After integration to get rid of the δ function and plus distributions, we find

$$\sigma_{ij}(\eta,m^2) = \int_{1-4(1+\eta)+4\sqrt{1+\eta}}^{1} dz \mathcal{H}(z,\alpha) \sigma_{ij}'(\eta,z,m^2). \quad (43)$$

The kernel of the hard part is

$$\mathcal{H}(z,\alpha) = 1 + \int_{0}^{\ln[1/(1-z)]} dx e^{E(x,\alpha)} \sum_{j=0}^{\infty} Q_j(x,\alpha). \quad (44)$$

The kernel in Eq. (44) depends solely on the resummation exponent $E(x,\alpha)$, either explicitly, or through the functions Q_j which depend exclusively on E. This exponent, in turn, depends on the factorization scheme, i.e., for the process under consideration, on Eqs. (17) and (18). It is to this exponent that we turn our attention in the next section.

III. THE RESUMMATION EXPONENT

Invoking universality with the Drell-Yan case, we can express the exponent for $t\bar{t}$ production using the results of Ref. [13]. By the same token, *because of the restrictions* on that universality we may keep only the pieces of the exponent that are universal in the two cases, i.e., the pieces that reproduce upon expansion the leading logarithmic structures attributable to initial-state radiation, exemplified in Eq. (17). The details of the inversion of the Mellin transform, expressed in Eq. (44), may be found in Refs. [11,12] and are analyzed further in Sec. IV.

In this section, we present the exponent $E(x,\alpha)$ of Eq. (44) in moment space, where the moment $n = \exp(x)$. For the Drell-Yan process, the exponent in moment space in the PVR approach may be written in either the DIS or the $\overline{\text{MS}}$ factorization scheme [10,14]. In the DIS scheme,

$$E(x,\alpha) = -\int_P d\zeta \frac{\zeta^{n-1}-1}{1-\zeta} \left\{ \int_{(1-\zeta)^2}^{(1-\zeta)} \frac{d\lambda}{\lambda} g_1[\alpha(\lambda m)] \right.$$
$$\left. + g_2\{\alpha[(1-\zeta)m]\} \right\}, \quad (45)$$

and, in the $\overline{\text{MS}}$ case,

$$E(x,\alpha) = -\int_P d\zeta \frac{\zeta^{n-1}-1}{1-\zeta} \int_{(1-\zeta)^2}^{1} \frac{d\lambda}{\lambda} g_1[\alpha(\lambda m)]. \quad (46)$$

Here P is a principal-value contour [10]; g_1 and g_2 are functions of the QCD running coupling strength $\alpha(\lambda m)$. It is important to note that Eqs. (45) and (46) include in general all large logarithmic structures in the Drell-Yan case. This exponent is renormalization-group invariant, by construction. The logarithmic structures generated by this exponent are recovered upon expanding the functions g_i as perturbative series with respect to the running coupling strength and re-expanding the running coupling strengths in terms of the hard-scale coupling strength $\alpha(m)$ [10]. As we argued in the general discussion of Sec. II B, and as shown explicitly in [10], a series of truncations can include all large threshold corrections.

The only necessary ingredients are the two-loop running coupling strength and a few terms in the expansions of the g_i's. In general, g_1 generates all the leading threshold corrections and some nonleading ones, and g_2 completes the resummation of numerically important nonleading ones. Since we base our resummation on universality, which is valid for leading logarithms only, we disregard g_2 for most of the rest of this paper, and we use the notation $g \equiv g_1$. We apply the consistency requirement of resumming leading logarithms only by performing the appropriate truncations and neglecting subleading structures whenever they appear. We describe these structures quantitatively in this section. We discuss the renormalization-group (RG) properties of resummation in Sec. III D. The process of resumming leading logarithms only, and the associated truncations, result in an approximation of the renormalization-group-invariant exponent of Eq. (45) by an exponent that is *approximately* renormalization-group invariant. By varying the factorization-renormalization scale μ within a logical range about its central value $\mu = m$, we obtain a variation of the resulting resummed cross section that serves as a quantitative measure of the effects of logarithmic structures that are not resummable in the $t\bar{t}$ process. Variation with μ is *the bulk* of the theoretical uncertainty.

A. Truncation and perturbative representation of the exponent

Using the truncations

$$g[\alpha(\lambda m)] = \sum_{j=1}^{\infty} \alpha^j(\lambda m) g^{(j)} \simeq \alpha(\lambda m) g^{(1)}, \quad (47)$$

along with

$$\alpha(\lambda m) = \frac{\alpha}{1+\alpha b_2 \ln\lambda}, \quad \alpha \equiv \alpha(m), \quad (48)$$

we write the PVR exponent in the $\overline{\text{MS}}$ scheme as

$$E(x,\alpha) \simeq -\alpha g^{(1)} \int_P d\zeta \frac{\zeta^{n-1}-1}{1-\zeta} \int_{(1-\zeta)^2}^{1} \frac{d\lambda}{\lambda} \frac{1}{1+\alpha b_2 \ln\lambda}. \quad (49)$$

This integral can be evaluated exactly [10]. The result is

$$E(x,\alpha) = -\frac{g^{(1)}}{b_2} \frac{1}{t} \sum_{m=1}^{\infty} \frac{(1-n)_m}{m! \, m^2} \mathcal{E}(mt), \quad (50)$$

where

$$t \equiv \frac{1}{2\alpha b_2}, \quad (1-n)_m = \frac{\Gamma(1-n+m)}{\Gamma(1-n)},$$

$$\mathcal{E}(y) = y e^{-y} \mathrm{Ei}(y), \tag{51}$$

and the exponential integral is defined by the principal value

$$\mathrm{Ei}(y) \equiv \mathcal{P} \int_{-\infty}^{y} dx\, e^x / x. \tag{52}$$

Equation (49) or, equivalently, Eq. (50) has a perturbative asymptotic representation [10]

$$E(x,\alpha) \simeq E(x,\alpha,N(t)) = g^{(1)} \sum_{\rho=1}^{N(t)+1} \alpha^\rho \sum_{j=0}^{\rho+1} s_{j,\rho} x^j. \tag{53}$$

This representation is valid in the moment-space interval

$$1 < x \equiv \ln n < t. \tag{54}$$

The coefficients are

$$s_{j,\rho} = -b_2^{\rho-1} (-1)^{\rho+j} 2^\rho c_{\rho+1-j} (\rho-1)!/j!, \tag{55}$$

and the constants c_k are obtained from the expansion $\Gamma(1+z) = \Sigma_{k=0}^{\infty} c_k z^k$, where Γ is the Euler gamma function.

The number of perturbative terms $N(t)$ in Eq. (53) is obtained by optimizing the asymptotic approximation

$$|E(x,\alpha) - E(x,\alpha,N(t))| = \text{minimum}. \tag{56}$$

Using Eqs. (50), (53), and (55), we rewrite Eq. (56) as

$$\left| \sum_{m=1}^{n} \frac{(1-n)_m}{m!\, m^2} \mathcal{E}(mt) - \sum_{\rho=0}^{N(t)} \frac{(-1)^\rho \rho!}{t^\rho} \sum_{j=0}^{\rho+2} \frac{(-1)^{j-1} c_{\rho+2-j}}{j!} x^j \right|$$

$$= \text{minimum}. \tag{57}$$

Equation (57) denotes an approximation between two functions of the moment n, and it determines the optimum number of perturbative terms N as a function of the parameter t. Indeed, as shown numerically below, within the interval of Eq. (54), the optimization of Eq. (57) has a solution that depends on t *only*, $N = N(t)$. It also can be shown [12] that in the complementary interval

$$t < x \equiv \ln n < \infty, \tag{58}$$

the approximation Eq. (55) breaks down for any integer N that is a function of t *only*. For very large n within the interval of Eq. (58) the asymptotic approximation

$$E(x,\alpha) \simeq -\frac{g^{(1)}}{b_2} \left\{ t\left(\frac{x}{t} - 1\right) \ln\left(\frac{x}{t} - 1\right) - x \right\} \tag{59}$$

holds, and it is clearly a nonperturbative one.

Throughout this paper, we use the two-loop formula for the fixed coupling strength

$$\alpha(m) \equiv \frac{\alpha_s(m)}{\pi} = \frac{1}{b_2 \ln(m^2/\Lambda^2)} - \frac{b_3}{b_2^3} \frac{\ln[\ln(m^2/\Lambda^2)]}{\ln^2(m^2/\Lambda^2)}, \tag{60}$$
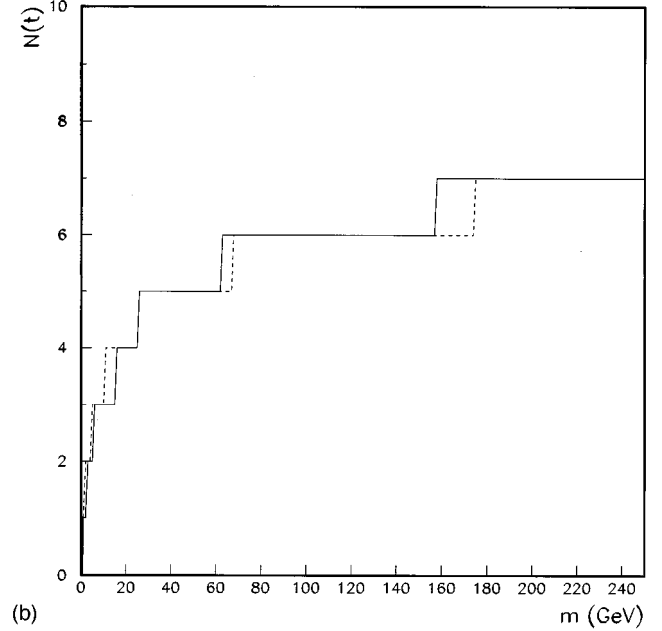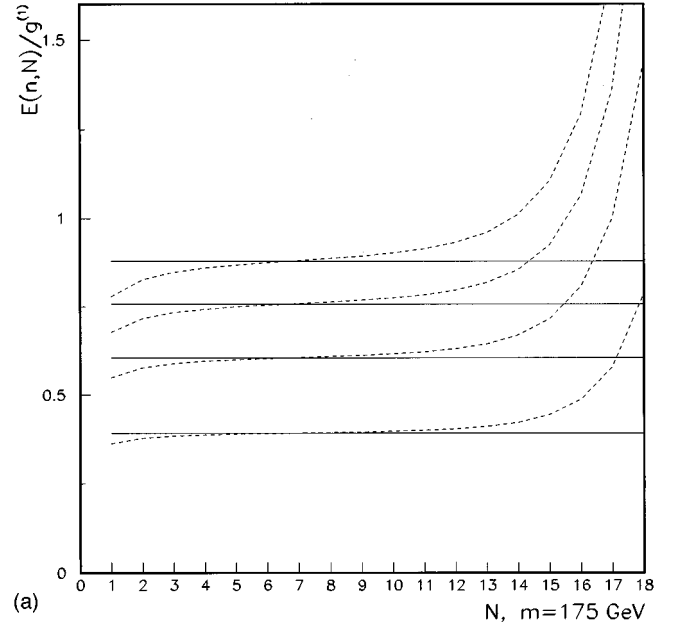
with

(a)

(b)

FIG. 1. Optimum number of perturbative terms in the exponent. (a) Normalized principal-value exponents (solid) and their perturbative approximations (dashed) as a function of N, for fixed mass and for four parametric moment values (from the bottom, at $n = 10, 20, 30, 40$). Optimization occurs at $N[t(m=175\ \text{GeV})] = 6$ for all four moments. (b) The function $N[t(m)]$ (solid) and its simple analytic approximation $[t(m) - 3/2]$ (dashed).

$$b_2 = (11C_A - 2n_f)/12,$$

$$b_3 = [34C_A^2 - (10C_A + 6C_F)n_f]/48, \tag{61}$$

and number of flavors $n_f = 5$. We set $\Lambda = 0.158$ GeV (the CTEQ3M value [15]).

In Fig. 1 we illustrate the validity of the asymptotic approximation for a value of t corresponding to $m = 175$ GeV. In Fig. 1(a) we show how $N(t)$ is determined from Eq. (57)

for a fixed t and selected parametric values of n. The plot shows that optimization works perfectly, and it demonstrates the typical breakdown of the asymptotic approximation as N increases beyond $N(t)$. This rise is the exponential rise of the infrared renormalons, the $\rho!$ growth in the second term of Eq. (57). As long as n is in the interval of Eq. (54), all the members of the family in n are optimized at the same $N(t)$, showing that the optimum number of perturbative terms is a function of t only. In Fig. 1(b) we plot the function $N(t)$ for a range of t relevant to $t\bar{t}$ production. An excellent numerical approximation is provided by the fit

$$N(t)\simeq[t-3/2],\qquad(62)$$

where the integer part is defined as the closest integer from either direction. [It is amusing that this fit suggests a lower limit for the hard scale m. A perturbative series is an improvement in accuracy if $N(t)\geq1$ which, from the above fit, implies $t-3/2\geq0.5$. Using for simplicity a one-loop fit of $\alpha(m)$ and Λ, we deduce that the hard scale $m/\Lambda\geq e^2\simeq8$, well within our expectations.]

Equations (54) and (57) suggest a perturbative behavior for the exponent in moment space *independently of* the color factors which reside in $g^{(1)}$. In particular, the range of validity of the perturbative expression for the exponent, $x/t<1$, is obtained by *direct comparison* with the exact principal-value definition, as shown in Fig. 2. [Equations (58) and (59) are also suggestive, but they constitute an asymptotic limit, valid for x larger than t.] This range of validity has the consequence that terms in the exponent of the form $\alpha^k\ln^k n$ are of order unity, and terms with fewer powers of logarithms, $\alpha^k\ln^{k-m}n$, are negligible. This explains why resummation is completed in a finite number of steps in the Drell-Yan process, as discussed earlier. The same is true here, but, in addition, we discard monomials $\alpha^k\ln^k n$ in the exponent because of the restricted universality between the $t\bar{t}$ and $l\bar{l}$ processes.

The exponent we use in the rest of the paper is the truncation

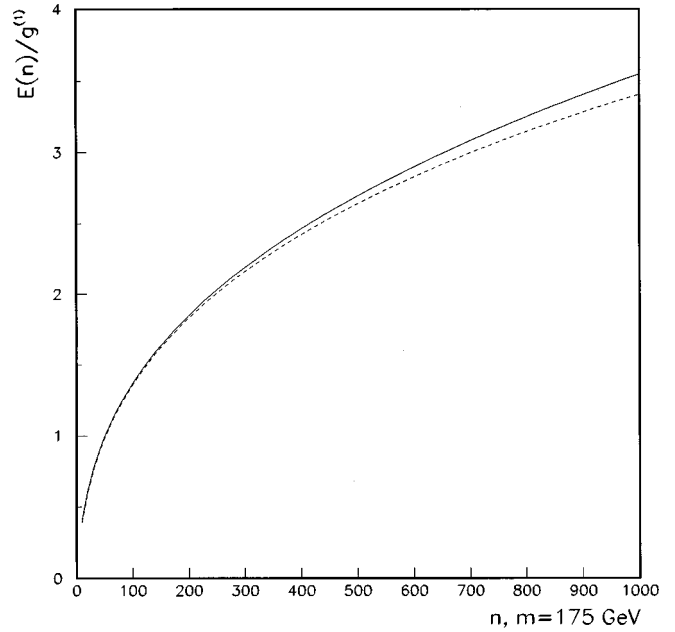$$E(x,\alpha,N)=g^{(1)}\sum_{\rho=1}^{N(t)+1}\alpha^\rho s_\rho x^{\rho+1},\qquad(63)$$

FIG. 2. The normalized principal-value exponent (solid) and its perturbative approximation (dashed) vs the moment, n.

with the coefficients

$$s_\rho\equiv s_{\rho+1,\rho}=b_2^{\rho-1}2^\rho/\rho(\rho+1).\qquad(64)$$

We note in passing that the leading-logarithm truncation of the exponent, Eqs. (63) and (64), forms a convergent series,

$$E(x,\alpha,N)\simeq\frac{g^{(1)}}{b_2}x\left\{1+\left(\frac{1}{2\alpha b_2 x}-1\right)\ln(1-2\alpha b_2 x)\right\},\qquad(65)$$

as long as $x<1/(2\alpha b_2)\equiv t$. This, of course, is not true for the exponent of Eq. (53) that contains the full subleading logarithmic structures in the Drell-Yan process. We use the convergent version of the exponent Eq. (65) in special cases to arrive at simplified expressions for the perturbative regime in momentum space.

There are equivalent expressions appropriate for the DIS factorization scheme. Equation (49) becomes

$$E(x,\alpha)\simeq-\alpha g^{(1)}\int_P d\zeta\frac{\zeta^{n-1}-1}{1-\zeta}\int_{(1-\zeta)^2}^{1-\zeta}\frac{d\lambda}{\lambda}\frac{1}{1+\alpha b_2\ln\lambda}=-\frac{g^{(1)}}{b_2}\left\{\frac{1}{t}\sum_{m=1}^\infty\frac{(1-n)_m}{m!m^2}\mathcal{E}(mt)-\frac{1}{2t}\sum_{m=1}^\infty\frac{(1-n)_m}{m!m^2}\mathcal{E}(2mt)\right\}.\qquad(66)$$

The perturbative approximation, subject to the truncation requirements discussed previously, is

$$E(x,\alpha,N)=g^{(1)}\sum_{\rho=1}^{N(t)+1}\alpha^\rho s_\rho x^{\rho+1}-g^{(1)}\sum_{\rho=1}^{N(2t)+1}\left(\frac{\alpha}{2}\right)^\rho s_\rho x^{\rho+1},\qquad(67)$$

or, in convergent form,

$$E(x,\alpha,N)\simeq\frac{g^{(1)}}{b_2}x\left\{\left(\frac{1}{2\alpha b_2 x}-1\right)\ln(1-2\alpha b_2 x)\right.$$
$$\left.-\left(\frac{1}{\alpha b_2 x}-1\right)\ln(1-\alpha b_2 x)\right\}.\qquad(68)$$

The convergent exponents, Eqs. (65) and (68), suggest the perturbative interval of Eq. (54), independently of PVR. On the other hand, beyond the end point $x=1/(2\alpha b_2)$ these con-

vergent expressions are ill defined because the leading term has a branch-point singularity.

B. Regularization-independence of the perturbative exponent

It is valuable to stress that we can derive the perturbative expressions, Eqs. (53), (54), (55), and (62), without the PVR prescription, although with less certitude. The analysis of this subsection is presented in order to show that our final perturbative results do not depend on the specific manner that the infrared region is regularized in the PVR approach.

We begin with the *unregularized* form of Eq. (49), i.e., with the integration over x done on the real axis:

$$E_0(x,\alpha) = -\alpha g^{(1)} \int_0^1 dx \frac{x^{n-1}-1}{1-x} \int_{(1-x)^2}^1 \frac{d\lambda}{\lambda} \frac{1}{1+\alpha b_2 \ln\lambda}. \tag{69}$$

We expand the inner integrand as a Taylor series around α. As we will see, part of the problem now transforms into ignorance of the asymptotic properties of this expansion. Writing

$$\int_{(1-x)^2}^1 \frac{d\lambda}{\lambda} \frac{1}{1+\alpha b_2 \ln\lambda} = 2\sum_{\rho=1} \frac{(-1)^\rho}{\rho t^{\rho-1}} \ln^\rho(1-x), \tag{70}$$

we deduce

$$E_0(x,\alpha) = -2\alpha g^{(1)} \sum_{\rho=1} \frac{(-1)^\rho}{\rho t^{\rho-1}} \int_0^1 \frac{dy}{y} [(1-y)^{n-1}-1] \ln^\rho y. \tag{71}$$

The upper limit of the summation in Eq. (71) is left undetermined, because, as is made evident below, the series represented is only formal, i.e., not convergent. Lack of convergence is associated with the Landau pole exhibited by the original integral, Eq. (69). Using the identity

$$\ln^\rho y = \lim_{\eta\to 0} \left(\frac{\partial}{\partial\eta}\right)^\rho y^\eta, \tag{72}$$

and the Stirling approximation for the beta function $B(n,\eta)$,

$$\lim_{\eta\to 0} \left(\frac{\partial}{\partial\eta}\right)^\rho \left(B(n,\eta) - \frac{1}{\eta}\right) = \rho! \sum_{j=0}^{\rho+1} \frac{(-1)^j}{j!} c_{\rho+1-j} \ln^\rho n, \tag{73}$$

we find

$$E_0(x,\alpha) = g^{(1)} \sum_{\rho=1} \alpha^\rho \sum_{j=0}^{\rho+1} s_{j,\rho} x^j, \quad x \equiv \ln n, \tag{74}$$

with the coefficients of Eq. (55). This expression for $E_0(x,\alpha)$ is the same as Eq. (53), the only and major difference being that we do not know the asymptotic properties of this series in the full range of moments n. The added information is precisely what is furnished by PVR, as we saw earlier. Both the function $N(t)$ *and* the range of validity of the perturbative expression, $1 < x \equiv \ln n < t$, are provided by the principal-value prescription.

To be more explicit, we examine Eq. (74) in some detail. Because the coefficients $s_{j,\rho}$ grow factorially, the series does

not represent a convergent infinite series for a fixed t and n. The factorial growth is precisely the infrared renormalon induced by the existence of the Landau-pole singularity of the original integral. Without this factorial, as in the truncated expression, Eq. (63), the resulting infinite series is convergent for a fixed n, but it diverges nevertheless at the threshold $n \to \infty$ due to the powers of the logarithm. Since E is the exponent of the cross section, the resulting singularities in the cross section would be essential singularities. In fact, in Eqs. (53) and (55) there is a tradeoff between factorial growth and powers of logarithms: greater factorial growth is accompanied by fewer powers of moment logarithms (and hence of momentum logarithms in the cross section).

We conclude that the nature of the series in Eq. (74) is asymptotic, and we rewrite Eq. (74) as

$$E_0(x,\alpha) \simeq E(x,\alpha,N) = g^{(1)} \sum_{\rho=1}^N \alpha^\rho \sum_{j=0}^{\rho+1} s_{j,\rho} x^j, \quad x \equiv \ln n. \tag{75}$$

Because the original integral is unregulated, the properties and range of validity of this asymptotic series are not obvious. In PVR, regularization is incorporated, and, since there are no undetermined extra scales, such as the introduction of IR cutoffs, the asymptotic properties are determinable fully, as shown in Sec. III A.

For a fixed t and n, one may use the monotonicity behavior of the corresponding partial sums to try to determine an upper limit for the number of terms in Eq. (75). This procedure is illustrated in Fig. 3(a) for $m = 175$ GeV. We note that beyond a certain range of N, the exponent increases factorially, a demonstration of both the asymptotic nature of the series and of the effect of the IR renormalons. A range of optimum N can be determined where the growth of the sum reaches a plateau, before the factorial growth sets in at large N. The exponent is fairly flat in this region so the indeterminacy of the optimum N is insignificant numerically. The plateau is centered around $N_{\text{opt}} \simeq 6$ to 7 for a wide range of moments, in agreement with the results of the previous subsection. One can make these statements quantitative by defining the slope

$$S(x,\alpha,N) \equiv \frac{\partial E(x,\alpha,N)}{\partial N} = E(x,\alpha,N+1) - E(x,\alpha,N). \tag{76}$$

For a range of n where there is a plateau, the optimum N can be determined by the equation

$$N_{\text{opt}} : S(x,\alpha,N)|_{x,\alpha=\text{fixed}} = \text{minimum}. \tag{77}$$

In Fig. 3(b), we observe that the optimization of the perturbative exponent with this method gives the same results as the principal-value method: i.e.,

$$N_{\text{opt}} - 1 \simeq N(t) = [t - 3/2]. \tag{78}$$

A second issue is whether one could determine the same range of validity, Eq. (54), of the representation Eq. (75) without PVR. This is possible if we impose the *supplementary* requirement that this representation results in a value of
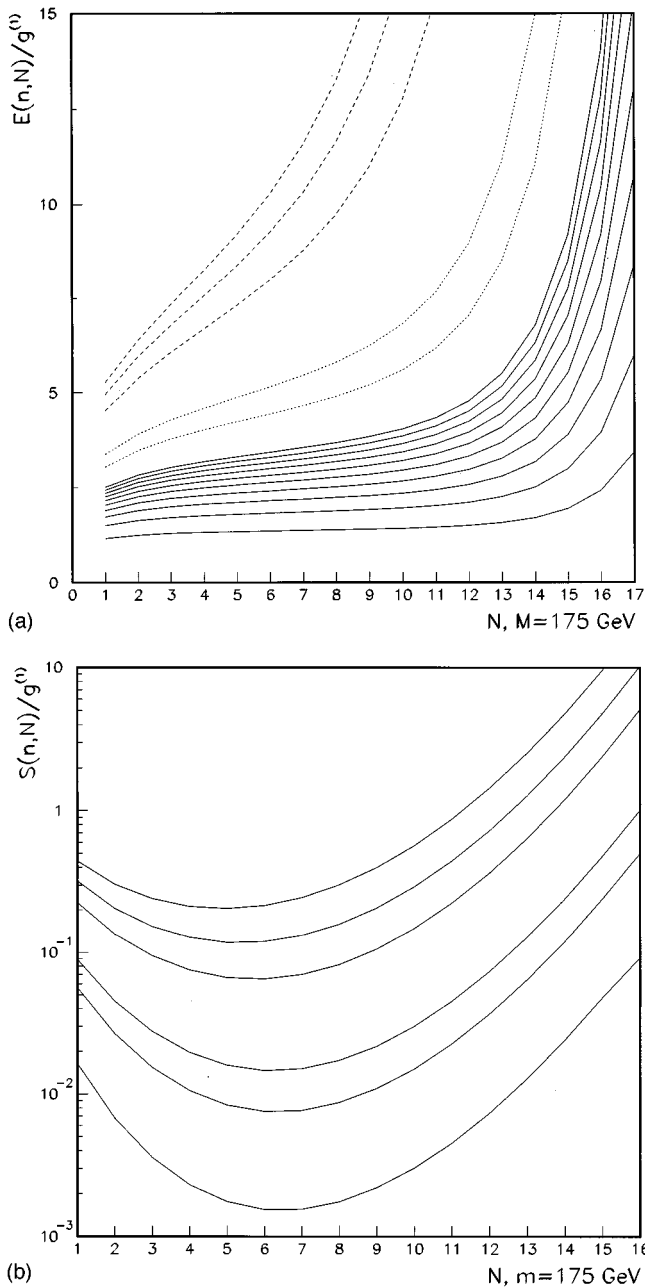
(a)

(b)

FIG. 3. The normalized perturbative exponent without regulators. (a) Partial sums vs the number N of terms as a parametric family in n: The solid bunch is for $n \in \{100,1000\}$ (increasing) in steps of 100. The dotted bunch is for $n = 2000,3000$ (increasing). The dashed bunch is for $n = 10\,000, 20\,000, 30\,000$ (increasing). (b) Slope function vs N for $n = 10, 50, 100, 500, 1000, 2000$ (increasing). The minimum is attained at $N - 1 \simeq N[t(m = 175 \text{ GeV})] = 6$, for $n \lesssim 1000 \simeq m/\Lambda$.

N_{opt} that depends *only on the hard scale* m, and not on the moment n. In Fig. 3(b) we show N_{opt}, the minimum of the slope $S(n,N)$ for various values of n at $m = 175$ GeV. We observe that N_{opt} is constant in approximately the same range of n as in Eq. (54). When n is increased beyond that range, the corresponding N_{opt} becomes a function of n. As n is increased, the plateau created by the corresponding values of the exponent starts shrinking, and the renormalons move to

the left of the figure. For values of n close to the boundary of Eq. (54), the slope in Eq. (76) becomes substantial.

The two requirements, a plateau in $E(x, \alpha, N)$ and a value of N_{opt} that depends only on the hard scale, allow one to make statements concerning the perturbative representation of the exponent that are similar to those the PVR approach, albeit with less certitude. The perturbative representation of the exponent, Eqs. (53), (54), (55), and (62), is obtained in straightforward fashion in PVR, but the analysis of this subsection shows that the result is approximately independent of the regularization PVR imposes. The result can be recovered by a study of the factorial growth of the partial sums and the reasonable physical requirement that the plateau of stability of the exponent depend on the hard scale of the problem only.

C. Perturbative regime of the hard part in moment space

We have established a perturbative representation for the exponent in moment space, with or without principal-value regularization. The conclusions are similar. The exponent has a perturbative representation in the range

$$1 < x \equiv \ln n < t \equiv \frac{1}{2 \alpha b_2} \tag{79}$$

independent of the constant $g^{(1)}$, i.e., of the channel-dependent color factors. This is a *maximum* range allowed for the perturbative cross section in moment space. One should distinguish, however, between the range in moment space where the exponent has a perturbative representation, and the range where the cross section itself is perturbative. The distinction arises because the cross section, which is proportional in moment space to the *exponential* of $E(\ln n, \alpha, N)$, is much more sensitive to variations in n. The cross section also depends exponentially on the color factors $g^{(1)}$, which can be much larger than unity, while the perturbative representation of the exponent in the regime of Eq. (79) is independent of the color factors.

We address the question of the perturbative regime in momentum space in Sec. IV, where we present the inverse Mellin transform that provides the cross section. However, one can furnish a heuristic argument in moment space as well. Again, this argument is independent of the regularization prescription of the original integral representation of the exponent, once we work with its asymptotic perturbative approximation, Eqs. (53) and (63).

The idea is to regard the plateau of Fig. 3(a) as a region of *perturbative stability* in both of the variables it depends on, namely N and n. Denote the kernel of the hard part in moment space by

$$\widetilde{I}(n, \alpha, N) = e^{E(\ln n, \alpha, N)}. \tag{80}$$

Then, this kernel is perturbatively stable in an interval of n such that variations around the center of the plateau $N(t)$, which does not depend on n in the perturbative regime, provide $O(\alpha_s)$ variations for $\widetilde{I}(n, \alpha, N)$, i.e., numerically negligible contributions that are not enhanced by threshold effects. This statement is made quantitative by the requirement

$$\delta_N \widetilde{I}(n,\alpha,N(t)) = e^{E(\ln n,\alpha,N(t))}\delta_N E(\ln n,\alpha,N(t))$$

$$= e^{E(\ln n,\alpha,N(t))}S(\ln n,\alpha,N(t)) \lesssim \alpha_s, \quad (81)$$

where the slope S is defined in Eq. (76). Another way of reaching the condition of Eq. (81) begins with the order-by-order perturbative hard part written as

$$\widetilde{I}^{[k]}(n,\alpha) = \sum_{m=0}^{k} \alpha^m s_m(n) + \sum_{m=1}^{k} \alpha^m r_m(n). \quad (82)$$

The first sum in Eq. (82) contains singular functions of n that produce large threshold enhancements and must be resummed, while the second sum contains regular functions of n, whose numerical effects are of $O(\alpha_s)$. The first sum is replaced by our resummed $\widetilde{I}(n,\alpha,N(t))$, and the condition in Eq. (81) is equivalent to a plateau of perturbative stability such that variations of the resummed terms around the plateau belong to the second, regular, sum of Eq. (82):

$$e^{E(\ln n,\alpha,N(t)) + \delta_N E(\ln n,\alpha,N(t))}$$

$$\simeq e^{E(\ln n,\alpha,N(t))} + e^{E(\ln n,\alpha,N(t))}S(n,\alpha,N(t))$$

$$\simeq e^{E(\ln n,\alpha,N(t))} + \sum_{m=1}^{l} \alpha^m r'_m(n), \quad (83)$$

so that $\delta_N \widetilde{I}(n,\alpha,N(t)) = O(\alpha_s)$. This is the same criterion as Eq. (81).

The regular sums in Eqs. (82) and (83), have been calculated only to first order in $t\bar{t}$ production. This is the reason

we consider them at most equal to α_s, rather than assuming definite numerical coefficients, large or small, unsupported by exact calculations. This statement is corroborated by the exact one-loop calculation of the $t\bar{t}$ cross section, and by the one- and two-loop calculations of the Drell-Yan cross section. It is in general assumed in all resummation procedures.

D. Renormalization-group properties of the perturbative exponent

We have studied the exponent under the simplification that the renormalization-factorization scale, the ''hard scale,'' is fixed at $\mu = m$. In this subsection, we discuss the dependence on μ of the resummation exponent in moment space. We work entirely in the $\overline{\text{MS}}$ scheme. Since RG invariance is one of the ingredients of resummation, we expect that the full Drell-Yan exponent, containing the full scale dependence, is exactly RG invariant. It can be seen by inspection that Eq. (46) is scale invariant:

$$E(x,\alpha) = E(x,\alpha(\mu),m/\mu)$$

$$= -\int_P d\zeta \frac{\zeta^{n-1}-1}{1-\zeta} \int_{(1-\zeta)^2 m^2/\mu^2}^{m^2/\mu^2} \frac{d\lambda}{\lambda} g_1[\alpha(\lambda\mu)]. \quad (84)$$

Here we ask to what degree the truncations we impose, starting from Eq. (49), affect this invariance. We begin with the explicitly μ-dependent equivalent of Eq. (49), read from Eq. (84). The corresponding expression is [14]

$$E(x,\alpha(\mu),m/\mu) \simeq -\alpha(\mu)g^{(1)}\int_P d\zeta \frac{\zeta^{n-1}-1}{1-\zeta} \int_{(1-\zeta)^2 m^2/\mu^2}^{m^2/\mu^2} \frac{d\lambda}{\lambda} \frac{1}{1+\alpha(\mu)b_2\ln\lambda}, \quad (85)$$

where the dependence on μ is both implicit [in $\alpha(\mu)$] and explicit. Working along the lines of Sec. III B, we may show that

$$E(x,\alpha(\mu),m/\mu) \simeq E(x,\alpha(\mu),m/\mu,N(\mu)) = -g^{(1)} \sum_{\rho=1}^{N(\mu)+1} \alpha^\rho(\mu) \frac{(-1)^\rho 2^\rho b_2^{\rho-1}}{\rho} \sum_{k=1}^{\rho} \frac{\rho!}{(\rho-k)!} \ln^{\rho-k}(m/\mu) \sum_{j=0}^{k+1} \frac{(-1)^j}{j!} c_{k+1-j} x^j. \quad (86)$$

We use the approximation $N(\mu) \simeq N[t(\mu)]$. This equation makes clear that *explicit* μ-variation (i.e., $k < \rho$) is equivalent to inclusion of *nonleading* logarithms x^j, $j < \rho+1$. In this sense, uncertainty expressed through μ variation overlaps with uncertainty expressed through inclusion of nonuniversal logarithms. In the triple sum of Eq. (86), the $k = \rho$ term is the numerically dominant term in the exponent. This term represents the implicit μ dependence, Eq. (53). All other $\ln(m/\mu)$ terms are nonleading in $x = \ln n$. The linear term in $\ln(m/\mu)$, obtained for $k = \rho-1$, has a universal $\ln n$ substructure. It is the one containing equal powers of $\alpha(\mu)$ and $\ln n$. It comes from the same diagrams as the leading $\ln n$ structures at $\mu = m$ and amounts to exponentiation of the explicit $O(\alpha_s^3)$ μ variation.

Our μ-dependent exponent for $t\bar{t}$ production can therefore be written

$$E(x,\alpha(\mu),m/\mu,N(\mu)) = g^{(1)}\left\{ \sum_{\rho=1}^{N(\mu)+1} \alpha^\rho(\mu) \frac{b_2^{\rho-1}2^\rho}{\rho(\rho+1)} x^{\rho+1} - \ln(m/\mu) \sum_{\rho=1}^{N(\mu)+1} \alpha^\rho(\mu) \frac{b_2^{\rho-1}2^\rho}{\rho} x^\rho \right\}. \quad (87)$$

We call attention to the sign structure of Eq. (87). For a fixed moment and scales μ decreasing from m, the implicit growth of the first sum due to the increase of $\alpha(\mu)$ is cancelled by the minus sign of the explicit dependence of the second sum, and vice versa. On the other hand, in the truncation from Eq. (86) to Eq. (87), nonuniversal subleading logarithmic structures are discarded. Therefore we expect only approximate scale invariance of Eq. (87).

In Fig. 4 we plot the normalized exponent, in each of the truncated versions of Eqs. (85), (86), and (87), versus a wide variation of $\mu \in \{100,300\}$ GeV, and for various perturbative values of the moment n. We see that both the PV Drell-Yan exponent, Eq. (85), and its perturbative Drell-Yan version, Eq. (86) are straight lines, practically coincident. The universal exponent, Eq. (87), is a gently increasing function of μ, and it lies somewhat below the Drell-Yan exponent. The increase creates a partial compensation of the explicit μ dependence of the Born cross sections, more so than if the full Drell-Yan exponent were used. This difference stands to reason, since no implicit μ dependence exists in the Drell-Yan process at the Born level. These μ-dependent properties conform to the intuition that our resummed cross section should show less variation with μ than the next-to-leading-order counterpart. We call attention to Fig. 4(b), where we show the effects of μ dependence as a function of the number of terms in the partial sums. For the Drell-Yan exponent, the addition of perturbative terms *up to the optimum number* $N[t(\mu)]$ makes the exponent progressively scale invariant.

Smooth behavior under scale transformations is not a property of the resummation of Ref. [3]. If an IR cutoff is used, conventional RG-scale invariance looses much of its meaning since an additional and arbitrary scale is introduced. We return to this issue in Sec. V when we discuss the physical cross section and compare scale variations in our approach with the corresponding ones of Ref. [3].

IV. LEADING AND SUBLEADING LOGARITHMIC STRUCTURES

In this section we describe the resummed partonic cross section in momentum space, derive a perturbative approximation in a specific region of momentum space, and discuss in general how to include leading logarithmic structures consistently in the resummation. We also demonstrate how the constant $g^{(1)}$ is determined from the one-loop calculation, and we discuss the issue of universality of the leading logarithms. In particular, we demonstrate that retention of subleading pieces in the exponent, of a structure similar to the Drell-Yan case, would not account correctly for the subleading structure at the one-loop level in top quark production. We justify the truncations we use consistently with universality of initial-state radiation.

The general form of the PVR cross section in the $\overline{\text{MS}}$ scheme is

$$\sigma_{ij}^{\text{PV}}(\eta,m^2) = \int_{1-4(1+\eta)+4\sqrt{1+\eta}}^{1} dz \mathcal{H}(z,\alpha)\sigma_{ij}'(\eta,z,m^2),$$

(88)

where the kernel of the hard part is

$$\mathcal{H}(z,\alpha) = 1 + \int_0^{x_z} dx e^{E(x,\alpha)} \sum_{j=0}^{\infty} Q_j(x,\alpha),$$

(89)

and

$$x_z \equiv \ln\left(\frac{1}{1-z}\right).$$

(90)

The functions $Q_j(x,\alpha)$ in Eq. (89) appear during the inversion of the Mellin transform $n \leftrightarrow z$ [11]. They are obtained from the generating function

$$\mathcal{Q}[P_1,P_2,\ldots,P_{N+1}] \equiv \text{Re}\left\{\frac{1}{i\pi}\sum_{m_1,m_2,\ldots,m_{N+1}=0}^{\infty}\frac{P_1^{m_1}P_2^{m_2}\cdots P_{N+1}^{m_{N+1}}}{m_1!m_2!\ldots m_{N+1}!}\lim_{\epsilon\to 0}\left(\frac{\partial}{\partial\epsilon}\right)^{m_1+2m_2+\cdots(N+1)m_{N+1}}e^{i\pi\epsilon}\Gamma(1+\epsilon)\right\}$$

(91)

through the identification

$$\mathcal{Q}[P_1,P_2,\ldots,P_{N+1}] \equiv \sum_{j=0}^{\infty} Q_j.$$

(92)

This notation is slightly different from that of Ref. [11]. In particular, in the present notation the real part is extracted explicitly from the generating function. In Eqs. (91) and (92),

$$P_k = P_k(x,\alpha) \equiv \frac{\partial^k E(x,\alpha)}{k!\partial x^k}.$$

(93)

The function $Q_j = Q_j(x,\alpha)$ is defined as the set of terms in Eq. (89) that contribute j more powers of α than of x. The

structures Q_j resum the jth subleading logarithms in the physical cross section through the index identity

$$j = \sum_{k=2} m_k(k-1)$$

(94)

that connects Eqs. (91) and (92).

A. The leading resummed perturbative cross section and its range of validity

For best accuracy, in a process like the Drell-Yan process, the expression for the hard part should include enough of the set of Q_j's to reproduce the resummable finite-order subleading logarithms up to two loops. On the other hand, owing to the constrained universality that characterizes the $t\bar{t}$ cross

section, we should include only terms that do not create non-universal subleading logarithms. In addition, we must discuss the range in momentum space where our perturbative resummation is valid.

We turn first to the issue of the perturbative regime in momentum space. Specification of this region follows from general expressions for the inversion of the Mellin transform and the meaning of the successive terms in this inversion, once their perturbative approximations are used. The kernel of the hard part is provided in Eq. (89), and the functions Q_0 and Q_1, obtained from Eqs. (91) and (93), are

$$Q_0 = \frac{1}{\pi}\sin(\pi P_1)\Gamma(1+P_1) \qquad (95)$$

and

$$Q_1 \simeq 2\Gamma(1+P_1)P_2\cos(\pi P_1)\Psi(1+P_1). \qquad (96)$$

The functions $\Psi \equiv \Psi^{(0)}$ and $\Psi^{(k)}$ are the usual polygamma functions. For simplicity we include in the expression for Q_1 only terms that generate corrections starting at $O(\alpha)$. According to the general discussion at the beginning of this section, Q_1 contributes one less power of x than of α in the integrand of Eq. (89), and it is formally subleading relative to the contribution of Q_0. Nevertheless, from Eqs. (95) and (96), we see that this suppression is not true for values of x such that $P_1(x,\alpha) \simeq 1$. When $\sin(\pi P_1) \simeq 0$, the dominance of Q_0 over Q_1 is destroyed. For values of x such that $P_1 > 1$, Q_0 and Q_1 are out of phase, with amplitudes that are not constrained, and the perturbative dominance of Q_0 over Q_1 is again vitiated.

We conclude that the perturbative region in momentum space is defined by the inequality constraint

$$P_1(x_z,\alpha) \lesssim 1. \qquad (97)$$

In our discussion in moment space in Sec. III, we saw that the perturbative approximation for the exponent is valid in the interval $1 < \ln n \lesssim t = 1/2\alpha b_2$, i.e., where terms containing equal powers of $\ln n$ and α are at most $O(1)$. Our Eq. (97) translates this condition consistently into momentum space. In Fig. 5 the upper two curves show the range in $\ln n = x$ where the constraint of Eq. (97) is satisfied. The lower three curves in Fig. 5 pertain to the corresponding constraint for the hard part in moment space, Eq. (81). We see that the two criteria are in good agreement: the value of $\ln n = x$ at which Eq. (97) is satisfied agrees fairly well with the value of n at which Eq. (81) is also.

We take up next the issue of universal logarithmic structures in our resummation. Power-counting, discussed generically in Sec. II B, must be altered when applied to the kernel of the integral in Eq. (89) because the extra integration supplies one more power of the logarithm. We begin with the following expression for the kernel of the hard part:

$$\mathcal{H}(z,\alpha) \simeq 1 + \int_0^{x_z} dx\, e^{E(x,\alpha)} Q_0(x,\alpha), \qquad (98)$$

and we rewrite
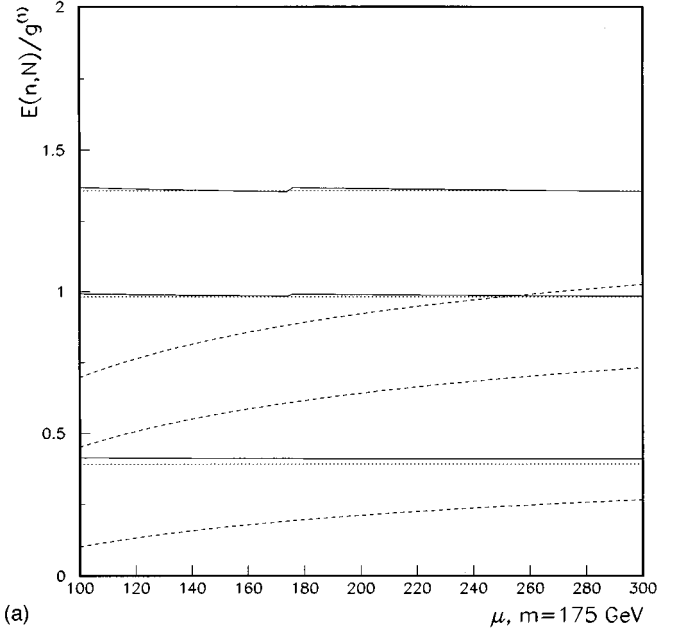
(a)
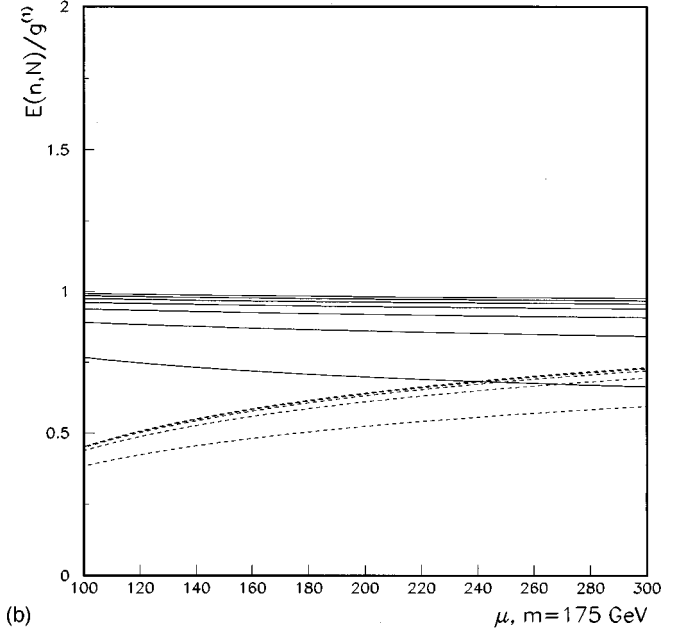
(b)

FIG. 4. Renormalization-factorization hard-scale dependence of the resummation exponents: (a) Drell-Yan perturbative (solid), principal value (dotted), and leading-logarithm (dashed) exponents vs μ for fixed mass and parametric moment values $n = 10,50,100$ (increasing); $N = N[t(m = 175 \text{GeV})] + 1$. (b) Parametric families of partial sums $N = 1, \ldots, N[t(m = 175 \text{GeV})] + 1$ (increasing) vs μ for the Drell-Yan (solid) and leading-logarithm (dashed) exponents, at $n = 50$.

$$Q_0(x,\alpha) = Q_0(x,\alpha) - P_1(x,\alpha) + P_1(x,\alpha)$$
$$\equiv \Delta(x,\alpha) + P_1(x,\alpha). \qquad (99)$$

Using Eq. (63), we can express

$$e^{E(x,\alpha)} = \sum_{m=0}^{\infty} \alpha^m \sum_{l=m+1}^{2m} \epsilon(l,m)x^l, \qquad (100)$$
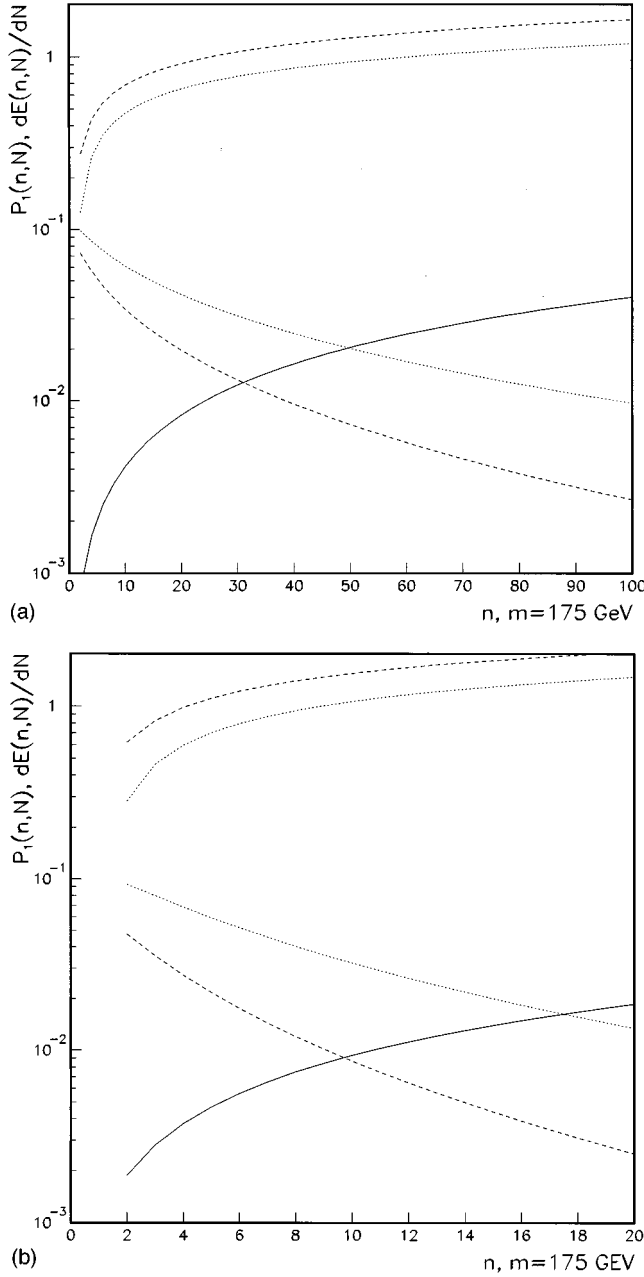
(a)
n, m=175 GeV

(b)
n, m=175 GEV

FIG. 5. Evaluation of the perturbative regime: (a) Saturation of the perturbative constraint in the $q\bar{q}$ channel as derived in moment space [$S(n)$, solid; $\alpha_s e^{-E(n)}$, dashed (Drell-Yan); dotted (leading logarithms)] and in momentum space [$P_1(n) \leq 1$; dashed, Drell-Yan; dotted, leading logarithms]; $N = N[t(m=175 \text{ GeV})]+1$. The upper curves are those in momentum space. (b) Same as in (a) but for the gg channel.

and, from the definitions of Q_0 and P_1, we find the expansion

$$\Delta(x,\alpha) = \sum_{m=2}^{\infty} \alpha^m \delta_m x^m. \qquad (101)$$

Therefore,

$$\int_0^{x_z} dx\, e^{E(x,\alpha)} \Delta(x,\alpha)$$

$$= \sum_{m=0}^{\infty} \alpha^{m+2} \sum_{k=0}^{m} \sum_{l=k+1}^{2k} \frac{\epsilon(l,k)\delta_{m+2-k}}{3+m+l-k} x_z^{3+m+l-k}. \qquad (102)$$

For a fixed m, the maximum monomial in powers of x_z is $\alpha^{2+m} x_z^{2m+3}$. In the notation of Sec. II B, the integral in Eq. (102) contributes *at most* to the first-subleading logarithms $c(2m-1,m)$. Since we intend to resum leading logarithms only, we ignore the contribution from the integral Eq. (102). For the same reason, we discard all Q_j's but Q_0 in Eq. (89).

Our main result for the perturbative resummed partonic cross section, denoted by $\sigma_{ij}^{\text{pert}}$, is, therefore,

$$\sigma_{ij}^{R,\text{pert}}(\eta,m^2) = \int_{1-4(1+\eta)+4\sqrt{1+\eta}}^{z_0} dz$$

$$\times \left[1 + \int_0^{x_z} dx\, e^{E(x,\alpha)} P_1(x,\alpha) \right] \sigma_{ij}'(\eta,z,m^2)$$

$$= \int_{1-4(1+\eta)+4\sqrt{1+\eta}}^{z_0} dz\, e^{E(x_z,\alpha)} \sigma_{ij}'(\eta,z,m^2). \qquad (103)$$

The upper limit of integration $z_0 \equiv z_0(\alpha)$ is determined from the equation for the perturbative regime

$$\frac{1}{1-z_0} = e^{x_0}, \quad P_1(x_0,\alpha) = 1. \qquad (104)$$

The preceding expressions in this subsection are valid in either factorization scheme. The only distinction is the value of the multiplicative constant $g^{(1)}$ in Eq. (64). This constant can be determined from a comparison of the $O(\alpha)$ expansion of the resummed partonic cross section with the finite-order calculation of Refs. [1,2].

It is useful for purposes of comparison to expand the cross section to $O(\alpha^2)$. In the $\overline{\text{MS}}$ factorization scheme, using Eqs. (63) and (64), we obtain

$$E^{[2]}(x,\alpha) = \alpha g^{(1)} x^2 + 2\alpha^2 g^{(1)} b_2 x^3/3. \qquad (105)$$

Substituting Eq. (105) into Eq. (103), we find that the corresponding finite-order part of the resummed cross section is

$$\sigma_{ij}^{[2]}(\eta,m^2)\big|_{\text{pert}} = \int_{1-4(1+\eta)+4\sqrt{1+\eta}}^{1} dz \left\{ 1 + \alpha g^{(1)} \ln^2\left(\frac{1}{1-z}\right) \right.$$

$$+ \alpha^2 \left[\frac{(g^{(1)})^2}{2} \ln^4\left(\frac{1}{1-z}\right) \right.$$

$$\left. \left. + \frac{2}{3} g^{(1)} b_2 \ln^3\left(\frac{1}{1-z}\right) \right] \right\} \sigma_{ij}'(\eta,z,m^2). \qquad (106)$$

To determine $g^{(1)}$, one can use the corresponding $O(\alpha)$ expression for the cross section from Ref. [3], or derive an

asymptotic formula near threshold ($\eta \to 0$) for the $O(\alpha)$ piece of the integration, Eq. (106), and compare with the corresponding explicit expression of Ref. [1]. The former is simpler for the present purposes. In Sec. IV B, we derive the asymptotic threshold formula to demonstrate universality issues. The result is

$$g^{(1)}_{\overline{\mathrm{MS}}} = 2C_{ij}, \quad C_{q\bar{q}} = C_F, \quad C_{gg} = C_A, \qquad (107)$$

the same as in the Drell-Yan case. Our Eq. (106), including the $O(\alpha^2)$ term, is identical to that of Ref. [3].

Similarly, in the DIS factorization scheme, using Eqs. (67) and (64), we derive

$$E^{[2]}(x,\alpha) = \alpha g^{(1)} x^2/2 + \alpha^2 g^{(1)} b_2 x^3/2. \qquad (108)$$

Hence the cross section to $O(\alpha^2)$ becomes

$$\sigma^{[2]}_{ij}(\eta, m^2)|_{\mathrm{pert}} = \int_{1-4(1+\eta)+4\sqrt{1+\eta}}^{1} dz \left\{ 1 + \alpha \frac{g^{(1)}}{2} \ln^2\left(\frac{1}{1-z}\right) \right.$$
$$+ \alpha^2 \left[\frac{1}{2} \left(\frac{g^{(1)}}{2} \right)^2 \ln^4\left(\frac{1}{1-z} \right) \right.$$
$$\left. \left. + \frac{1}{2} g^{(1)} b_2 \ln^3\left(\frac{1}{1-z} \right) \right] \right\} \sigma'_{ij}(\eta, z, m^2). \qquad (109)$$

By comparison with the corresponding $O(\alpha)$ piece of Ref. [3], we obtain

$$g^{(1)}_{\mathrm{DIS}} = 2C_{ij} = g^{(1)}_{\overline{\mathrm{MS}}}, \qquad (110)$$

again in agreement with the Drell-Yan case. As before, Eq. (109), including the $O(\alpha^2)$ term, is identical to that of Ref. [3].

We close this subsection with simplified analytical expressions for the perturbative regime of the cross section, Eq. (97). For this purpose, we may use the convergent expressions, Eqs. (65) and (68). In the $\overline{\mathrm{MS}}$ factorization scheme, we obtain

$$P_1(x_z, \alpha) \simeq -\frac{g^{(1)}}{b_2} \ln(1 - 2\alpha b_2 x_z) \lesssim 1, \qquad (111)$$

and, in the DIS scheme,

$$P_1(x_z, \alpha) \simeq -\frac{g^{(1)}}{b_2} \ln(1 - 2\alpha b_2 x_z) + \frac{g^{(1)}}{b_2} \ln(1 - \alpha b_2 x_z) \lesssim 1. \qquad (112)$$

To obtain transparent analytical expressions, we specialize here to the one-loop approximation

$$2\alpha b_2 = \ln^{-1}(m/\Lambda). \qquad (113)$$

We obtain

$$1 - z \gtrsim \left(\frac{\Lambda}{m} \right)^{1 - \exp(-b_2/g^{(1)})} \quad \overline{\mathrm{MS}}, \qquad (114)$$

$$1 - z \gtrsim \left(\frac{\Lambda}{m} \right)^{1 - \exp(-b_2/g^{(1)})/2[1 - \exp(-b_2/g^{(1)})/2]} \quad \mathrm{DIS.} \qquad (115)$$

We observe that the nonperturbative regime is suppressed mainly by Λ/m to the first power, with a correction that depends on the color factors of the partonic production process. For $m = 175$ GeV,

$$\Lambda/m \simeq 10^{-3}. \qquad (116)$$

Because b_2 is positive ($b_2 \simeq 2$), the nonperturbative regime is an increasing function of the color factors. If the partonic cross sections had no color factor enhancements, $g^{(1)} \lesssim 1$, Eqs. (114) and (115) would be in close agreement with the perturbative regime of the exponent in moment space $n \lesssim m/\Lambda$, Eq. (54), with the direct substitution $1/n \leftrightarrow 1-z$. For example, for $g^{(1)} = 1$,

$$1 - z \gtrsim 2 \times 10^{-3} \quad \overline{\mathrm{MS}}$$

and

$$1 - z \gtrsim 1.5 \times 10^{-3} \quad \mathrm{DIS}, \qquad (117)$$

in good agreement with Eq. (116). In reality, $g^{(1)} = 8/3$ in the $q\bar{q}$ channel, therefore

$$1 - z \gtrsim 2 \times 10^{-2} \quad \overline{\mathrm{MS}}$$

and

$$1 - z \gtrsim 8 \times 10^{-3} \quad \mathrm{DIS}. \qquad (118)$$

For the gg channel, $g^{(1)} = 6$, and we find

$$1 - z \gtrsim 1 \times 10^{-1} \quad \overline{\mathrm{MS}}$$

and

$$1 - z \gtrsim 5 \times 10^{-2} \quad \mathrm{DIS}. \qquad (119)$$

These regions are narrower than the estimate based on the perturbative properties of the exponent only, especially for the gg channel. The soft-gluon region is probed more deeply in the DIS scheme than in the $\overline{\mathrm{MS}}$ scheme, closer to Λ/m. We discuss these properties numerically in Sec. V.

B. Nonuniversal subleading logarithms

In this subsection, we address universality of the logarithmic structures in the threshold region more explicitly. It is sufficient to examine the issue in the $\overline{\mathrm{MS}}$ scheme. For completeness, and to compare with the analytical results of Ref. [1], we derive the near-threshold asymptotic properties of the $O(\alpha)$ term of Eq. (106). We demonstrate that if we were to keep the subleading logarithm in the Drell-Yan exponent, Eqs. (53) and (55), the resulting term in the $O(\alpha)$ expansion of Eq. (89) would not be the same as the one obtained in the explicit next-to-leading order calculation of Ref. [1]. This is a demonstration of the consistency requirements of the series of truncations that resulted in Eqs. (63), (64), and (103).

In the $\overline{\text{MS}}$ scheme, Eq. (53), the full $O(\alpha)$ Drell-Yan exponent is

$$E^{[1]}(x,\alpha) = \alpha g^{(1)}(s_{2,1}x^2 + s_{1,1}x + s_{0,1}), \qquad (120)$$

where the coefficients are found in Eq. (55). Suppose we allow an undetermined linear term, $\alpha\kappa x$, that would represent the deviation of this exponent from the Drell-Yan form. We discard the constant term in this exercise, because it does not contribute logarithmic terms to the cross section at first

order. Substituting from Eq. (55) we have

$$E^{[1]}(x,\alpha) \simeq \alpha(g^{(1)}x^2 + 2g^{(1)}\gamma x + \kappa x), \qquad (121)$$

where γ is the Euler-Mascheroni constant. The kernel of the hard part, containing subleading logarithmic structures, is given generally by Eq. (89). To account for subleading logarithms with full accuracy in the Drell-Yan case, we must keep Q_0 and Q_1, Eqs. (95) and (96). Expanding to $O(\alpha)$ and substituting into Eq. (88), we obtain

$$\sigma_{ij}^{(1)}(\eta,m^2) = \alpha \int_{1-4(1+\eta)+4\sqrt{1+\eta}}^{1} dz \left[g^{(1)}\ln^2\left(\frac{1}{1-z}\right) + \kappa \ln\left(\frac{1}{1-z}\right) \right] \sigma'_{ij}(\eta,z,m^2). \qquad (122)$$

The piece of the Drell-Yan expression linear in the logarithm has dropped out. In other words, the exact evaluation of the cross section of Eq. (122) with the Drell-Yan resummation expression gives the same answer as the truncated expression, Eq. (106). This is something well known in the Drell-Yan case and is expressed by absence of the function g_2 in the $\overline{\text{MS}}$ scheme, Eq. (46).

The integral representation of the partonic cross section does not contain the subleading logarithms of the Drell-Yan case. This is not true for its asymptotic evaluation near threshold, as we shall see below, owing to the form of the Born cross section. We focus on the $q\bar{q}$ channel only. From Eqs. (20) and (122), we obtain

$$\sigma_{q\bar{q}}^{(1)}(\eta,m^2) = \frac{8}{9}\pi^3\alpha^3\frac{\tau}{s}\int_{1-4(1+\eta)+4\sqrt{1+\eta}}^{1} dz[1-(1-z)\tau]\left[\sqrt{[1-(1-z)\tau]^2-4\tau} + \frac{2\tau}{\sqrt{[1-(1-z)\tau]^2-4\tau}} \right]$$

$$\times \left[g^{(1)}\ln^2\left(\frac{1}{1-z}\right) + \kappa\ln\left(\frac{1}{1-z}\right) \right], \qquad (123)$$

where $\tau \equiv m^2/s$. Introducing the variables $x = [1-(1-z)\tau]^2 - 4\tau$ and [1] $\beta^2 = 1-4\tau$, we derive

$$\sigma_{q\bar{q}}^{(1)} = \frac{4}{9s}\alpha_s^3 \int_0^{\beta^2} dx[x^{1/2} + (1-\beta^2)x^{-1/2}/2]\left[g^{(1)}\ln^2\left(\frac{4}{1-\beta^2}[1-\sqrt{1-(\beta^2-x)}]\right) + \kappa\ln\left(\frac{4}{1-\beta^2}[1-\sqrt{1-(\beta^2-x)}]\right) \right]. \qquad (124)$$

The threshold is exhibited at $\beta \to 0$. Expanding

$$1 - \sqrt{1-(\beta^2-x)} \simeq (\beta^2-x)/2, \qquad (125)$$

and using

$$\ln^k x = \lim_{\epsilon \to 0}\left(\frac{\partial}{\partial\epsilon}\right)^k x^\epsilon, \qquad (126)$$

we find

$$\sigma_{q\bar{q}}^{(1)} \simeq \frac{4}{9}\alpha_s^3\frac{\beta^3}{m^2}\left\{ g^{(1)}\left(\frac{\partial}{\partial\epsilon}\right)^2\left(\frac{2\beta^2}{1-\beta^2}\right)^\epsilon \left[B(3/2,1+\epsilon) + \frac{1-\beta^2}{2\beta^2}B(1/2,1+\epsilon) \right] \right.$$

$$\left. + \kappa\frac{\partial}{\partial\epsilon}\left(\frac{2\beta^2}{1-\beta^2}\right)^\epsilon\left[B(3/2,1+\epsilon) + \frac{1-\beta^2}{2\beta^2}B(1/2,1+\epsilon) \right] \right\}. \qquad (127)$$

After computing the derivatives, we obtain

$$\sigma_{q\bar{q}}^{(1)} \simeq \frac{4}{9}\alpha_s^3\frac{\tau}{m^2}\beta^3\left[g^{(1)}\left\{\ln^2\left(\frac{2\beta^2}{1-\beta^2}\right)\left(B(3/2,1)+\frac{1-\beta^2}{2\beta^2}B(1/2,1)\right)\right.\right.$$

$$+2\ln\left(\frac{2\beta^2}{1-\beta^2}\right)\left(B(3/2,1)[\Psi(1)-\Psi(5/2)]+\frac{1-\beta^2}{2\beta^2}B(1/2,1)[\Psi(1)-\Psi(3/2)]\right)$$

$$\left.+B(3/2,1)([\Psi(1)-\Psi(5/2)]^2+\Psi'(1)-\Psi'(5/2))+\frac{1-\beta^2}{2\beta^2}B(1/2,1)([\Psi(1)-\Psi(3/2)]^2+\Psi'(1)-\Psi'(3/2))\right\}$$

$$\left.+\kappa\left\{\ln\left(\frac{2\beta^2}{1-\beta^2}\right)\left(B(3/2,1)+\frac{1-\beta^2}{2\beta^2}B(1/2,1)\right)+B(3/2)[\Psi(1)-\Psi(5/2)]+\frac{1-\beta^2}{2\beta^2}B(1/2,1)[\Psi(1)-\Psi(3/2)]\right\}\right].$$

$$(128)$$

Discarding the nonlogarithmic pieces and using the relations $\Psi(1)=-\gamma$, $\Psi(3/2)=-\gamma-\ln4+1$, we observe that all the coefficients of the logarithms can be rational. Introducing [1] $\rho=4\tau$, we end with

$$\sigma_{q\bar{q}}^{(1)}\simeq\frac{\alpha_s^3}{m^2}\frac{\beta\rho}{9}\{g^{(1)}\ln^2(8\beta^2)-[2g^{(1)}-\kappa]\ln(8\beta^2)\}. \tag{129}$$

Our Eq. (129) may be compared with the result of Ref. [1] in the $\overline{\text{MS}}$ scheme, denoted $\alpha_s^3 f_{q\bar{q}}^{(1)}$:

$$\alpha_s^3 f_{q\bar{q}}^{(1)}\simeq\frac{\alpha_s^3}{m^2}\frac{\beta\rho}{9}\left\{\frac{8}{3}\ln^2(8\beta^2)-\frac{41}{6}\ln(8\beta^2)\right\}. \tag{130}$$

We conclude that, for the leading logarithm,

$$g^{(1)}=8/3=2C_F, \tag{131}$$

the same value found in Eq. (107). However, for the next-to-leading linear logarithm,

$$2g^{(1)}=16/3\neq41/6. \tag{132}$$

A nonzero value for κ would be required. This exercise shows that universality between the Drell-Yan case and $t\bar{t}$ production is restricted to the leading logarithms only, as must be the resummation of these structures. The subleading logarithms in the full exponent of Eq. (53) are uncertain.

The analysis of this subsection justifies our truncated expressions, and it motivates several equivalent ways to define a quantitative measure of the overall theoretical uncertainty. The most straightforward is to vary the renormalization-factorization (hard) scale within a reasonable range and to use the variation of the cross section as a measure of the non-universal subleading structures. It is important to recall, however, that truncation of the resummation of leading logarithms at a given *higher order* produces subleading logarithms at that order, as the $O(\alpha^2)$ terms in Eqs. (106) and (109) show. We will assume that these particular subleading logarithms are approximately universal because they come from the evolution properties of the resummed universal leading logarithms of lower orders. This is true for the $\overline{\text{MS}}$ Drell-Yan cross section at two loops [16].

To summarize, the resummation exponent in the perturbative regime in the $\overline{\text{MS}}$ factorization scheme is

$$E(x,\alpha(\mu),m/\mu,N(\mu))=2C_{ij}\left\{\sum_{\rho=1}^{N[t(\mu)]+1}\alpha^\rho(\mu)\frac{b_2^{\rho-1}2^\rho}{\rho(\rho+1)}x^{\rho+1}-\ln(m/\mu)\sum_{\rho=1}^{N[t(\mu)]+1}\alpha^\rho(\mu)\frac{b_2^{\rho-1}2^\rho}{\rho}x^\rho\right\}. \tag{133}$$

In the DIS factorization scheme, it is

$$E(x,\alpha(\mu),\mu,N[t(\mu)])=2C_{ij}\left\{\sum_{\rho=1}^{N[t(\mu)]+1}\alpha^\rho(\mu)\frac{b_2^{\rho-1}2^\rho}{\rho(\rho+1)}x^{\rho+1}-\ln(m/\mu)\sum_{\rho=1}^{N[t(\mu)]+1}\alpha^\rho(\mu)\frac{b_2^{\rho-1}2^\rho}{\rho}x^\rho\right\}$$

$$-2C_{ij}\left\{\sum_{\rho=1}^{N[2t(\mu)]+1}\alpha^\rho(\mu)\frac{b_2^{\rho-1}}{\rho(\rho+1)}x^{\rho+1}-\ln(m/\mu)\sum_{\rho=1}^{N[2t(\mu)]+1}\alpha^\rho(\mu)\frac{b_2^{\rho-1}}{\rho}x^\rho\right\}. \tag{134}$$

The upper integer in the two sums is $N[t(\mu)] = [t(\mu) - 3/2]$, and $t(\mu) \equiv 1/[2\alpha(\mu)b_2]$. The perturbative resummed cross section in the corresponding scheme is obtained from the general expression, Eq. (89), within the region defined by Eq. (97). This restriction can be incorporated if we define z_0 through

$$P_1\left[\ln\left(\frac{1}{1-z_0(\mu,m/\mu)}\right), \alpha(\mu), m/\mu, N[t(\mu)]\right] = 1.$$

(135)

Imposing the constraint that only leading logarithms are resummed, we arrive at our *perturbative* resummed cross section

$$\sigma_{ij}^{R,\text{pert}}(\eta,m^2,\mu^2) = \int_{1-4(1+\eta)+4\sqrt{1+\eta}}^{z_0(\mu,m/\mu)} dz$$
$$\times e^{E(x_z,\alpha(\mu),m/\mu,N[t(\mu)])}\sigma_{ij}'(\eta,z,m^2).$$

(136)

The derivatives of the Born cross sections, $\sigma_{ij}'(\eta,z,m^2)$, are found in Eqs. (20) and (22).

We use the formulas above to calculate our predictions for the perturbative resummed cross section. The rest of the phase space in Eq. (136), from $z=z_0$ to the threshold $z=1$, is nonperturbative, and we declare ignorance about the cross section in that region. (In Sec. VI we engage in some speculations on nonperturbative physics.) A measure of the dominance of the universal logarithmic structures and their resummation in the perturbative regime in our approach is provided by the change in the cross section when the renormalization-factorization scale is varied within a reasonable range around the ''central'' value $\mu=m$. This variation measures the importance of subleading logarithmic structures that are nonuniversal and nonresummable in this approach. We use variation with μ as a working hypothesis for the bulk of the perturbative uncertainty [5].

V. THE RESUMMED CROSS SECTION

In this section we present analytical and numerical results for the resummed cross sections. Section V A is devoted to the partonic cross sections as functions of the variable η, while in Sec. V B we present the physical cross sections obtained after convolution of the partonic cross sections with parton densities. We furnish details on the technicalities involved, both kinematical and numerical. In Sec. V C we make comparisons with the predictions of Laenen, Smith, and van Neerven [3,4], denoted LSvN.

A. Partonic cross sections

The resummed partonic cross section has the form

$$\sigma_{ij}^{R,\text{pert}}(\eta,m^2,\mu^2) = \int_{1-4(1+\eta)+4\sqrt{1+\eta}}^{z_0(\mu,m/\mu)} dz$$
$$\times e^{E(x_z,\alpha(\mu),m/\mu,N[t(\mu)])}\sigma_{ij}'(\eta,z,m^2).$$

(137)

The upper limit of integration, $z_0(\mu,m/\mu)$, is provided by Eq. (135). For physical but relatively large values of η, the lower limit of integration may become negative, unlike the Drell-Yan process in which $0 < z < 1$. In this situation, far away from threshold, resummation of initial-state gluon radiation is irrelevant, and we do not perform resummation outside the range $0 < z < 1$. Finding the roots of the lower limit of integration in Eq. (137) we see that this equation is unconstrained for

$$\eta \leq (1+\sqrt{2})^2/4 - 1 = 0.457\,106\,8.$$

(138)

Equation (138) defines the region in phase space in which threshold effects are important. Above this value of η, Eq. (137) should be constrained so that it includes *only* the phase space where gluon radiation is produced near threshold.

In order to achieve the best accuracy available we wish to include in our predictions as much as is known theoretically. The exact next-to-leading order (one-loop) cross section is known [1,2], but the full two-loop calculation does not exist. Thus the best we can do at present is to include the full content of the one-loop partonic cross section along with our resummation of the leading logarithms to all orders. In so doing, we include both nonuniversal one-loop subleading logarithms and constants. This procedure is in common with previous resummations of this process [3] and the Drell-Yan process [12]. Our ''final'' resummed partonic cross section can therefore be written [5]

$$\sigma_{ij}^{\text{pert}}(\eta,m^2,\mu^2) = \sigma_{ij}^{R,\text{pert}}(\eta,m^2,\mu^2) - \sigma_{ij}^{(0+1)}(\eta,m^2,\mu^2)|_{R,\text{pert}}$$
$$+ \sigma_{ij}^{(0+1)}(\eta,m^2,\mu^2).$$

(139)

The second term is the part of the partonic cross section up to one loop that is included in the resummation, while the last term is the exact one-loop cross section [1,2].

For numerical purposes it is best to convert the ''improper'' integrations induced in Eq. (137) by the form of the Born cross sections, $\sigma_{ij}'(\eta,z,m^2)$ [see Eqs. (20) and (22)], to integrations without a numerical (but analytically integrable) singularity. This is achieved by the transformation

$$x = \sqrt{1 - \frac{4\tau}{[1-\tau(1-z)]^2}}.$$

(140)

In addition, it is easier to parametrize the perturbative regime z_0 by the moment variable n_0:

$$\frac{1}{1-z_0} = n_0, \quad n_0 = e^{x_0},$$

(141)

where x_0 is the first root of the equation

$$P_1(x_0(\mu,m/\mu),\alpha(\mu),m/\mu,N[t(\mu)]) = 1.$$

(142)

Taking into account the constraint on η, Eq. (138), we can write the various pieces of Eq. (139) as

$$\sigma_{ij}^{R,\text{pert}}(\eta,m^2,\mu^2) = \int_{L(\tau)}^{U(\tau,n_0)} dx\, e^{E(y(x),\alpha(\mu),m/\mu,N[t(\mu)])}\widetilde{\sigma}_{ij}(x),$$

(143)

where

$$U[\tau,n_0(\mu,m/\mu)]\equiv\sqrt{1-\frac{4\tau}{[1-\tau/n_0(\mu,m/\mu)]^2}},$$

$$\text{(144)}$$

$$L(\tau)\equiv\Theta\left(\frac{1}{(1+\sqrt{2})^2}-\tau\right)\sqrt{1-\frac{4\tau}{(1-\tau)^2}},\quad\text{(145)}$$

and

$$y(x)=\ln\left(\frac{\tau\sqrt{1-x^2}}{\sqrt{1-x^2}-2\sqrt{\tau}}\right).\qquad\text{(146)}$$

The second term in Eq. (139) is obtained from Eq. (143) by expanding the exponential up to $O(\alpha)$. The exponents for the two factorization schemes are found in Eqs. (133) and (134), while the transformed functions $\widetilde{\sigma}_{ij}(x)$ are

$$\widetilde{\sigma}_{q\bar{q}}(x)=\frac{32}{3}\pi^3\alpha^2\frac{\tau^{3/2}}{s}\left(\frac{1+x^2}{(1-x^2)^{5/2}}\right),\qquad\text{(147)}$$

and

$$\widetilde{\sigma}_{gg}(x)=\frac{1}{2}\pi^3\alpha^2\frac{\tau^{1/2}}{s}\frac{1}{(1-x^2)^{3/2}}\left[-\left(\frac{4}{3}x^2+5\tau+\frac{12\tau}{1-x^2}\right)x^2\right.$$
$$+\left(2x^4-\frac{8}{3}x^2+3\tau x^2+2-3\tau\right)x\ln\left(\frac{1+x}{1-x}\right)$$
$$\left.+\left(-\frac{8}{3}x^4-4x^2+\tau x^2+\frac{4}{3}-3\tau\right)\right].\qquad\text{(148)}$$

In Fig. 6 we show the perturbative boundary $n_0(\mu,m/\mu)$, obtained from Eqs. (141) and (142), as a function of the hard scale μ, for $m=175$ GeV. The scale μ is an artifact of perturbation theory, and μ variation is associated with truncation of the perturbative expansion. In a resummation such as ours, all significant perturbative knowledge of threshold effects is exhausted (all large perturbative threshold corrections are included), and the perturbative regime we calculate should also be insensitive to artifacts such as μ. Therefore, one expects the perturbative boundary to be independent of the hard scale μ and to depend only on the physical scale characterizing the threshold, m. We observe that the full Drell-Yan exponent produces a function P_1 that is almost exactly hard-scale invariant, establishing that our resummation conforms to this intuition. On the other hand, the truncation to universal logarithmic structures that we use for our predictions shows some scale dependence.

In Fig. 7 we show the resummed partonic cross sections $\sigma_{ij}^{\text{pert}}$ as a function of η, for $\mu=m$ and $m=175$ GeV, for both production channels in the $\overline{\text{MS}}$ factorization scheme. We choose a logarithmic scale in η to expand the threshold region. We also show the lowest-order and next-to-leading-order counterparts. The three curves differ substantially in the partonic threshold region $\eta<1$, with the final resummed curve exceeding the other two. Above $\eta\simeq1$, our resummed cross sections are essentially identical to the next-to-leading-order cross sections, as is to be expected since the near-threshold enhancements that concern us in this paper are not relevant at large η. In both the $q\bar{q}$ and the gg channels, we
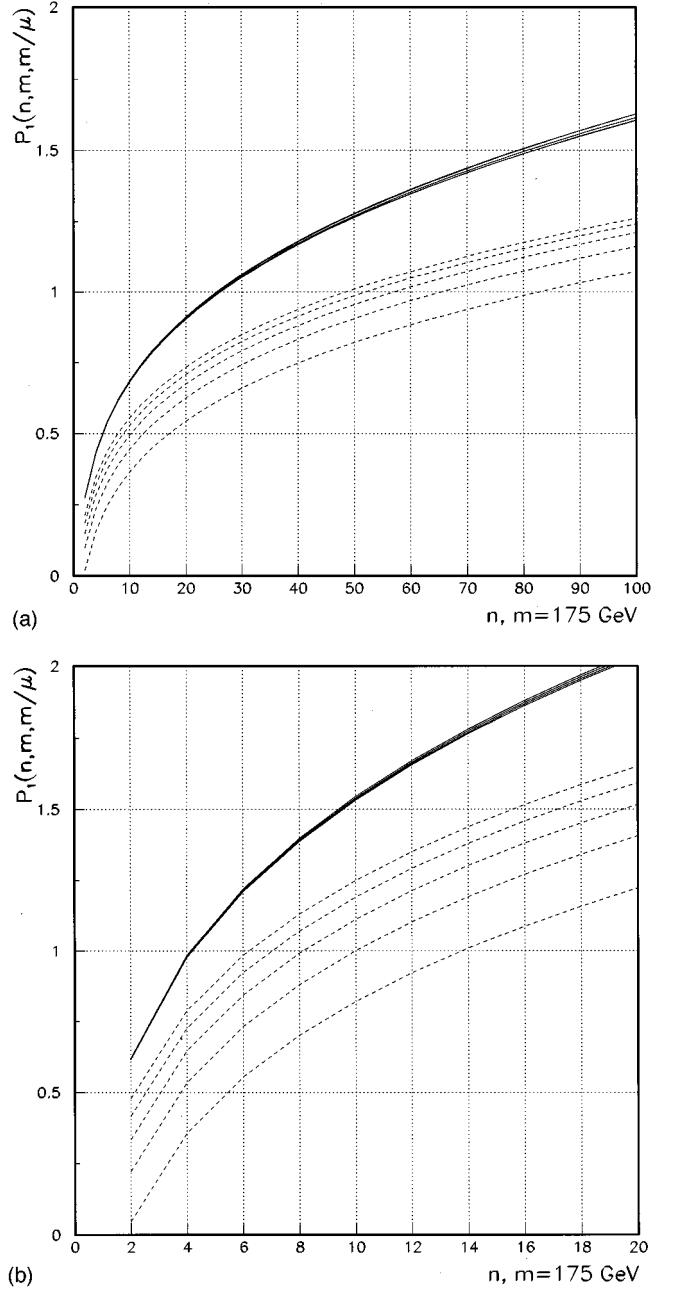

FIG. 6. Hard-scale dependence of the perturbative regime: (a) The function $P_1(n)$ vs n as a parametric family for $\mu=100,150,200,250,300$ GeV for the Drell-Yan exponent (solid bunch) and the leading-logarithm exponent (dashed bunch, decreasing) for the $q\bar{q}$ channel. (b) Same as in (a) for the gg channel.

note that the size of the $O(\alpha_s^3)$ term exceeds that of the $O(\alpha_s^2)$ term for $\eta\simeq0.1$, and the ratio grows as η decreases. This behavior is contrary to the notion underlying perturbation theory, that successive terms in the perturbation series should be smaller, and is cited in our Introduction as the motivation for resummation at small η.

It is useful to translate our definition of the perturbative regime directly into a statement about the perturbative region in η. Our perturbative resummation probes the threshold down to the point
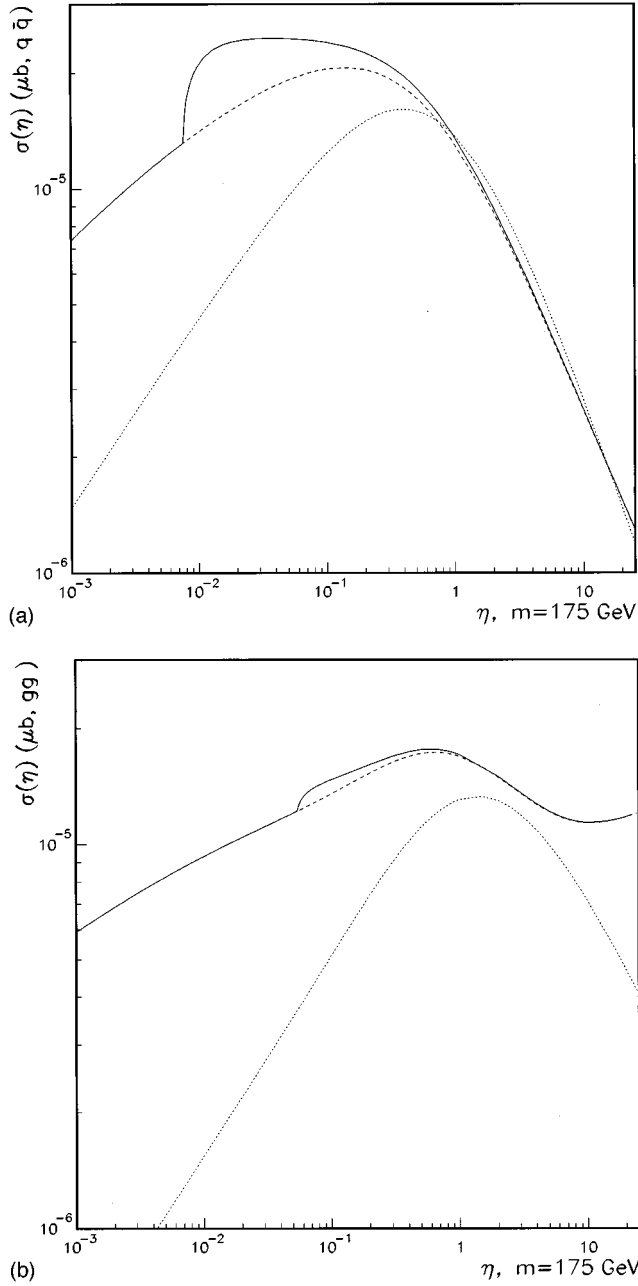
(a)

(b)

FIG. 7. The partonic cross sections $\sigma(\eta)$ as a function of η: (a) Born (dotted), next-to-leading order (dashed), and resummed (solid) partonic cross sections for the $q\bar{q}$ channel. (b) Same as in (a) for the gg channel.

$$\eta \geq \eta_0 = \frac{1}{2n_0}, \tag{149}$$

where n_0 is calculated from Eqs. (141) and (142). Below this value, perturbation theory, resummed or otherwise, is not to be trusted. For our central predictions we choose to accept the exact next-to-leading-order results throughout the phase space, but the nonperturbative region is a source of nonperturbative uncertainty, subject to model building. At $m = 175$ GeV, our resummed cross sections become identical to the next-to-leading-order cross sections below $\eta \geq 0.008$ for the $q\bar{q}$ channel and $\eta \geq 0.05$ for the gg channel, a consequence

of our decision to restrict resummation to the perturbative domain. The difference reflects the larger color factor in the gg case.

We return to possible nonperturbative contributions in Sec. VI.

B. The physical cross sections

We use S to denote the square of the hadronic center-of-mass energy. Once the partonic cross sections are calculated, the physical cross section for each production channel is obtained through the factorization theorem

$$\sigma_{ij}(S,m^2) = \frac{4m^2}{S} \int_0^{(S/4m^2)-1} d\eta$$

$$\times \Phi_{ij}\left[\frac{4m^2}{S}(1+\eta),\mu^2\right]\sigma_{ij}(\eta,m^2,\mu^2). \tag{150}$$

The parton flux is a convolution of parton distributions

$$\Phi_{ij}[y,\mu^2] = \int_y^1 \frac{dx}{x} f_{i/h_1}(x,\mu^2) f_{j/h_2}(y/x,\mu^2). \tag{151}$$

We use CTEQ3 parton distributions [15] in the appropriate factorization scheme. The total physical cross section is obtained after incoherent addition of the contributions from the $q\bar{q}$ and gg production channels. We ignore the small contribution from the qg channel.

A quantity of phenomenological interest is the differential cross section

$$\frac{d\sigma_{ij}(S,m^2,\eta)}{d\eta} = \frac{4m^2}{S} \Phi_{ij}\left[\frac{4m^2}{S}(1+\eta),\mu^2\right]\sigma_{ij}(\eta,m^2,\mu^2). \tag{152}$$

The differential distribution is a RG-invariant quantity, and it is perhaps measurable. Its integral over η is, of course, the total cross section. In Fig. 8 we plot these distributions for the two production channels for $m = 175$ GeV, $\sqrt{S} = 1.8$ TeV and $\mu = m$. Convolution with the parton flux enhances the relative importance of the region of small η. We observe that, at the energy of the Tevatron, resummation is significant for the $q\bar{q}$ channel and less so for the gg channel. Figure 8 is useful for back-of-the-envelope estimates of possible contributions from the nonperturbative regime, discussed in Sec. VI.

We show the total $t\bar{t}$-production cross section for various energies in Fig. 9, and in Table I we provide numerical values. The central value of our predictions is obtained with the choice $\mu/m = 1$, and the lower and upper limits are our estimate of the perturbative uncertainty. These upper and lower values are the maximum and minimum of the cross section in the range of the hard scale $\mu/m \in \{0.5,2\}$. For the range of top-quark mass shown, the minimum occurs at $\mu/m = 2$, while the maximum occurs at $\mu/m \simeq 0.7$, as is also shown in Fig. 9(b). Our prediction of Fig. 9(a) is in good agreement with the published data [17]. The μ variation of our resummed cross section, shown in Fig. 9(b) is smaller than that of the next-to-leading-order cross section, as expected for an
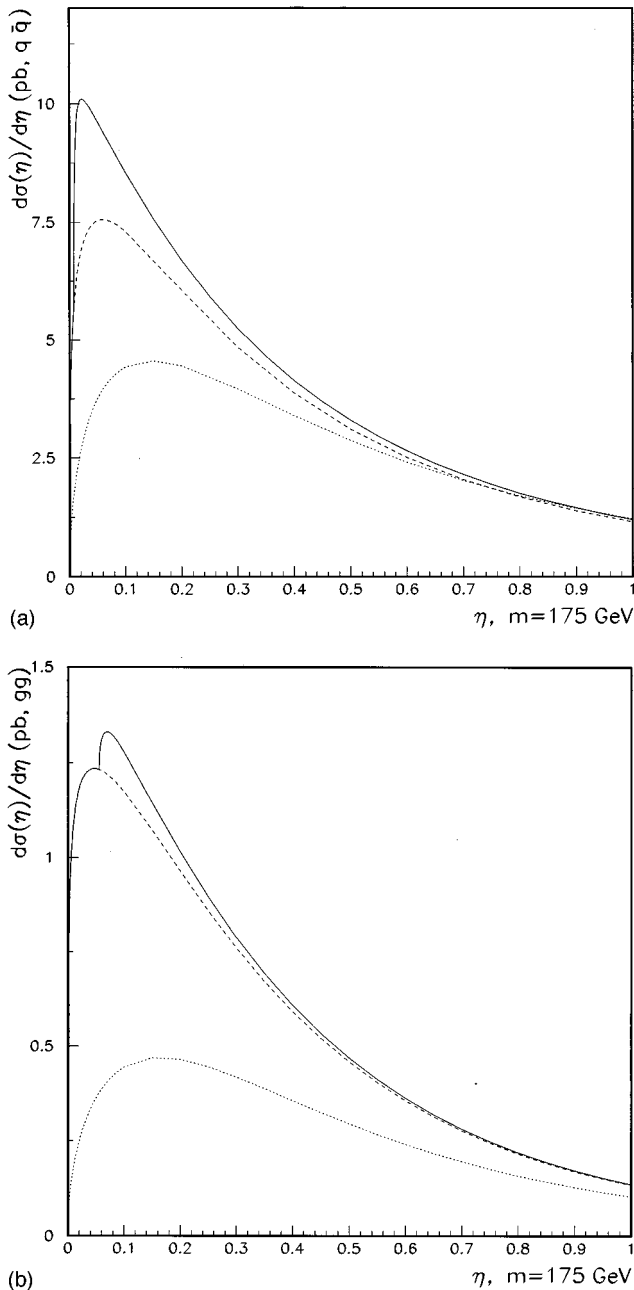
only leading-logarithmic threshold contributions are included in successive orders in α. We take the universal leading-logarithmic contributions at $O(\alpha)$ above the Born level from the full next-to-leading order calculations of $t\bar{t}$ production and the leading-logarithmic contributions at $O(\alpha^2)$ from calculations of the Drell-Yan cross section. For this exercise only, we set aside our perturbative constraint, Eq. (135), and instead we integrate over the entire threshold region $0 < z < 1$. We present the resulting finite order physical cross sections in the $\overline{\text{MS}}$ scheme in Fig. 10. (For the Born cross section, we integrate over all z.) We observe that the cross section $\sigma^{(0+1)}$ obtained from the leading-logarithm terms, only, through $O(\alpha)$ is in remarkable agreement with the cross section obtained from our full next-to-leading-order calculation for $t\bar{t}$ production. Moreover, our predicted resummed cross section lies part way between $\sigma^{(0+1)}$ and the cross section $\sigma^{(0+1+2)}$ obtained from the leading-logarithm terms, only, through $O(\alpha^2)$. At $m = 175$ GeV, the increase of $\sigma^{(0+1)}$ over the Born result is a 22% effect, and the further increase of $\sigma^{(0+1+2)}$ over $\sigma^{(0+1)}$ is another 14% effect. We conclude that the roughly 9% increase of our final resummed cross section above the next-to-leading order cross section is quite reasonable. It would be surprising if it were much less.

As remarked earlier in the paper, our resummation includes only the universal logarithmic structures. It is reasonable to inquire whether and by how much the predicted cross section would change if subleading logarithmic structures are included. One good representation of the possible effect of subleading structures is the full Drell-Yan exponent itself, Eq. (86). As shown in Fig. 4, this exponent is larger than our leading exponent, but the corresponding perturbative regime, calculated through Eq. (135), is smaller. To obtain a cross section that includes the Drell-Yan subleading logarithms we use Eqs. (88)–(90) with the sum over Q_j's replaced by the full first term, Q_0. It is shown as the dashed line in Fig. 11 for the $q\bar{q}$ channel. We see that the curves differ little from each other, and that the Drell-Yan resummation prediction is within our uncertainty band. This example substantiates our belief that μ variation is an adequate measure of perturbative uncertainty and that it includes the effect of nonresummable, nonuniversal logarithms.

A second source of uncertainty, that is partly phenomenological, partly perturbative, and partly correlated with non-universal logarithms, is associated with the use of different parton distributions. The parton set we use is a next-to-leading-order determination of the quark and gluon densities. Since we use resummed partonic cross sections, it is arguably true that we should also use parton densities based on resummed expressions for deep-inelastic lepton scattering cross sections and other processes used in the determination of the densities. However, no such densities exist. It is common practice phenomenologically to repeat calculations with different sets of parton and to estimate thereby a second source of uncertainty. Except for the fact that different data sets are used, or are emphasized differently, in different determinations of parton densities, and that the fitting programs differ, we opine that the practice of adding in quadrature, or otherwise, uncertainties associated with μ variation and those associated with different parton sets involves signifi-

FIG. 8. Differential cross section $d\sigma/d\eta$ as a function of η in the $\overline{\text{MS}}$ factorization scheme. The physical cross sections are the areas under the curves. (a) $q\bar{q}$ channel: Born (dotted), next-to-leading order (dashed), and resummed (solid). The nonperturbative regime is the area from $\eta = 0$ to the point in η at which the solid and dashed curves intersect. (b) Same as in (a) for the gg channel.

all-orders resummation. [Owing to a computer compiler error, the variation with μ of the next-to-leading-order results in the first paper of Ref. [5] is incorrect. Our overall resummed predictions are essentially unchanged. The dependence on μ shown in Fig. 9(b) is the correct variation.]

Our resummed cross sections at $\sqrt{S} = 1.8$ TeV are about 9% above their next-to-leading-order counterparts computed with the same parton distributions. To gain numerical insight into the magnitude of this increase, we may examine the growth of the cross section in the dominant $q\bar{q}$ channel that would be expected in a series of fixed-order calculations if
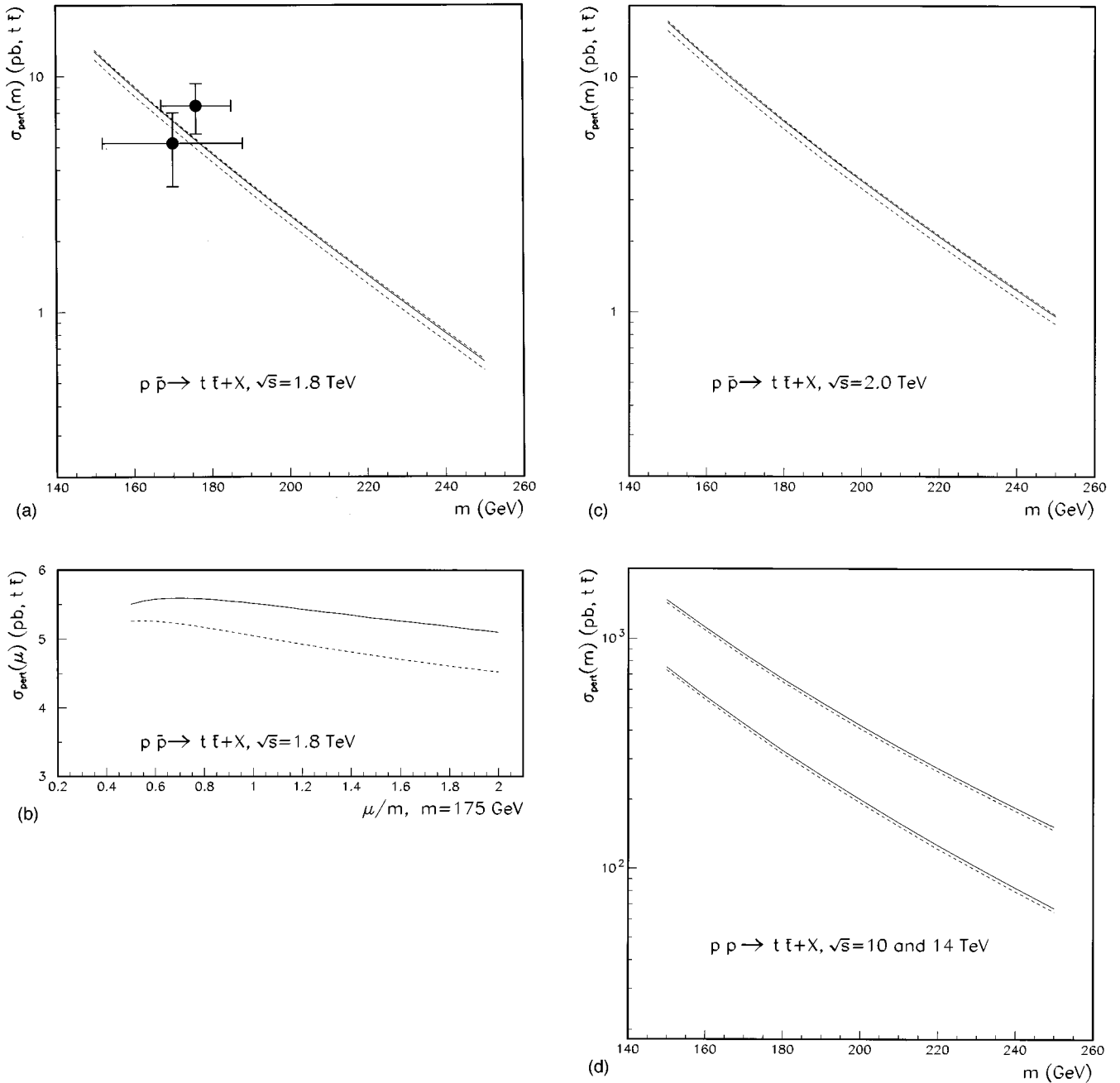
FIG. 9. Inclusive cross section for top-quark production in the $\overline{\text{MS}}$ scheme: (a) At the Tevatron, for $p\bar{p}\to t\bar{t}X$ at $\sqrt{S}=1.8$ TeV. The extremum dashed lines are our band of uncertainty, and the solid line between them is our central-value prediction. We also reproduce the published data of the CDF and D0 Collaborations. (b) Hard-scale dependence of the resummed (solid) and next-to-leading-order (dashed) cross sections at $\sqrt{S}=1.8$ TeV for $m=175$ GeV. (c) Same as in (a), but for the upgraded Tevatron, $\sqrt{S}=2.0$ TeV. (d) Central values of the resummed cross section (solid) for $pp\to t\bar{t}X$ at the CERN LHC energies of 10 and 14 TeV and the corresponding next-to-leading-order predictions (dashed).

cant double counting. Much of the difference among modern parton sets reduces to a difference in Λ which largely affects $\alpha(\mu)$. Thus, this difference is correlated with the μ variation we consider above, and should not be treated as an independent error. Over the range $\mu/m \in \{0.5,2\}$, the band of variation of the strong coupling strength α_s is a generous $\pm 10\%$ at $m = 175$ GeV.

In Fig. 9(c) we present our predictions for an upgraded Tevatron operating at $\sqrt{S}=2$ TeV. Our cross section is larger than the next-to-leading order one by about 9%. We predict

$$\sigma^{t\bar{t}}(m=175 \text{ GeV}, \sqrt{S}=2 \text{ TeV})=7.56^{+0.10}_{-0.55} \text{ pb}.$$

(153)

At $m=175$ GeV, the value of the cross section at $\sqrt{S}=2$ TeV is about 37% greater than that at $\sqrt{S}=1.8$ TeV.

Turning to pp scattering at the energies of the Large Hadron Collider (LHC) at CERN, we note a few significant differences from $p\bar{p}$ scattering at the energy of the Fermilab Tevatron. The dominance of the $q\bar{q}$ production channel at

TABLE I. The total $t\bar{t}$ production cross section at $\sqrt{S}=1.8$ TeV and its perturbative uncertainty. The theoretical error band, normalized with respect to the central value, represents an almost constant uncertainty of 9–10%.

m (GeV)	$\sigma_{\text{pert}}^{t\bar{t}}$ (min; pb)	$\sigma_{\text{pert}}^{t\bar{t}}$ (central; pb)	$\sigma_{\text{pert}}^{t\bar{t}}$ (max; pb)
150	11.76	12.72	12.90
155	9.87	10.68	10.83
160	8.33	9.01	9.14
165	7.06	7.63	7.73
170	6.00	6.48	6.57
175	5.10	5.52	5.59
180	4.36	4.71	4.78
185	3.73	4.04	4.09
190	3.20	3.46	3.51
195	2.75	2.98	3.02
200	2.37	2.57	2.60
205	2.04	2.21	2.24
210	1.77	1.91	1.94
215	1.53	1.65	1.68
220	1.32	1.43	1.45
225	1.15	1.24	1.26
230	0.99	1.08	1.10
235	0.86	0.94	0.96
240	0.75	0.81	0.83
245	0.65	0.71	0.72
250	0.57	0.62	0.63

the Tevatron is replaced by gg dominance at the LHC. Owing to the much larger value of $\sqrt{S}$, the near-threshold region in the subenergy variable is relatively less important, reducing the significance of initial-state soft-gluon radiation. Lastly, physics in the region of large partonic subenergy $\sqrt{s}$, where straightforward next-to-leading-order QCD is also inadequate [18], may become more significant for $t\bar{t}$ production at LHC energies than the effects of initial-state radiation. The approach of our paper is limited to the resummation of initial-state gluon radiation only. We present estimates in Fig. 9(d) of the cross section for LHC energies of 10 and 14 TeV. We obtain

$$\sigma^{t\bar{t}}(m=175 \text{ GeV}, \sqrt{S}=14 \text{ TeV})=760 \text{ pb}. \quad (154)$$

C. Comparisons with other calculations

In earlier sections we comment on differences between our formalism and that of Laenen, Smith, and van Neerven (LSvN) [3,4]. Here we compare aspects of our numerical predictions. The comparison most relevant to experiment is that of our Table I and the corresponding table in Ref. [4]. Our central values are 10–14 % larger (the difference increases with mass), and our estimated theoretical uncertainty is 9–10 % compared with their 28–20 % (decreasing with mass). The two predictions have overlapping uncertainties and are, in this sense, in agreement. In commenting on differences, we remark that our Born cross section is about 3–5 % larger than LSvN's Born cross section. The difference arises from the different parton distributions used in the two calculations, including differences in Λ which alone ac-

count for half or more of this increase. This source of difference should be kept in mind when comparisons are made with next-to-leading-order calculations and various previous results.

It is important to stress that the theoretical uncertainties are estimated in quite different ways in the two methods. We use the standard μ variation, whereas LSvN obtain their uncertainty primarily from variations of their undetermined IR cutoffs. From a theoretical point of view, a study of the variation of the cross section with the hard-scale μ is important because it deals with stability of the calculation under variation of a perturbative, but not directly determinable renormalization-factorization scale. This statement applies as well to the LSvN calculation, above and beyond the choice of their IR cutoff. The role of the IR cutoff is to measure ignorance of nonperturbative effects in the LSvN approach. One of the advantages of a resummation calculation should be diminished dependence of the cross section on μ, less variation than is present in fixed-order calculations.

It is also instructive to compare the numerical values of our perturbative boundary, $\eta_0(m,\mu/m)$, with the corresponding cut in η produced by LSvN's IR cutoff μ_0. In the $\overline{\text{MS}}$ scheme, their cut is [3]

$$\eta(\mu_0,\mu)=\frac{1}{2}\left(\frac{\mu_0}{\mu}\right)^3, \quad (155)$$

and in the DIS scheme it is

$$\eta(\mu_0,\mu)=\frac{1}{2}\left(\frac{\mu_0}{\mu}\right)^2. \quad (156)$$

Values of $\eta(\mu_0,\mu)$ are provided in Tables II and III and are compared with our perturbative boundary $\eta_0(m,\mu/m)$.

In the paragraphs to follow, we compare μ variation, scheme dependence, and the influence of the difference between our perturbative boundary and LSvN's cut in η. In Tables II and III, we reproduce numbers from Ref. [3] and show the corresponding values we calculate. The comparison is made at $m=100$ GeV in Table II because it is at this value of the top mass that they provide results in the $\overline{\text{MS}}$ scheme for both the $q\bar{q}$ and gg channels.

Tables II and III show that our resummed cross sections satisfy the test of stability under variation of the hard scale μ. The resummed results show less variation than the next-to-leading-order cross section. On the other hand, this is not true of the resummation of Ref. [3]. This distinction is linked to the absence of undetermined IR cutoffs in our method and the specific RG-invariant exponent we use. Both of these differences contribute to the instability apparent in the results of Ref. [3]. The LSvN results show less variation with μ in the DIS scheme than in the $\overline{\text{MS}}$ scheme, the reason they provide their final predictions in the DIS scheme. As shown in Table III, the variation with μ of their $q\bar{q}$ cross section in the DIS scheme is about 21%. For comparison, the next-to-leading-order cross section shows a variation of 9% and our resummed cross section a variation of 6%.

Our perturbative boundary, $\eta_0(\mu)$, is fairly insensitive to μ variation. In the $\overline{\text{MS}}$ scheme, it changes by about 30% around its central value (for $\mu=m$) while μ itself changes by 50–100 % from the central value. In the DIS scheme the

TABLE II. Physical cross sections in pb for $m = 100$ GeV at $\sqrt{S} = 1.8$ TeV. The LSvN predictions are shown for various choices of their IR cutoff μ_0. Our perturbative boundary η_0 and LSvN's phase-space cut $\eta(\mu_0,\mu)$ are also shown. Absences in the LSvN entries denote extremely large numbers.

$\sigma_{q\bar{q}}(m = 100$ GeV; $\overline{\text{MS}})$	$\mu/m = 0.5$	$\mu/m = 1$	$\mu/m = 2$
Born	64.3	48.4	37.3
NLO	54.6	55.0	51.3
$\sigma_{q\bar{q}}^{\text{pert}}$	56.9	59.4	57.2
LSvN($\mu_0 = 0.1m$)	52.6	88.9	-
LSvN($\mu_0 = 0.2m$)	42.5	66.4	110.5
$\eta_0(\mu)$	0.007	0.011	0.014
$\eta(\mu_0 = 0.1m,\mu)$	0.004	0.0005	0.000063
$\eta(\mu_0 = 0.2m,\mu)$	0.032	0.004	0.0005

$\sigma_{gg}(m = 100$ GeV; $\overline{\text{MS}})$	$\mu/m = 0.5$	$\mu/m = 1$	$\mu/m = 2$
Born	36.4	23.8	16.1
NLO	44.5	40.5	34.0
$\sigma_{gg}^{\text{pert}}$	44.8	41.6	35.0
LSvN($\mu_0 = 0.2m$)	34.3	88.7	-
LSvN($\mu_0 = 0.3m$)	28.1	42.4	820.0
$\eta_0(\mu)$	0.036	0.063	0.1
$\eta(\mu_0 = 0.2m,\mu)$	0.032	0.004	0.0005
$\eta(\mu_0 = 0.3m,\mu)$	0.108	0.0135	0.0017

$\sigma_{t\bar{t}}(m = 100$ GeV; $\overline{\text{MS}})$	$\mu/m = 0.5$	$\mu/m = 1$	$\mu/m = 2$
Born	100.7	72.2	53.4
NLO	99.1	95.5	87.4
$\sigma_{t\bar{t}}^{\text{pert}}$	101.7	101.0	92.2
LSvN($\mu_0 = \{0.2,0.3\}m$)	70.6	108.8	930.5

changes in $\eta_0(\mu)$ are even smaller, ranging from 16 to 28 %. The mild changes in $\eta_0(\mu)$ accord with our earlier physical expectation that the boundary is characteristic of the particle's mass, not of the perturbative artifact μ. If a complete resummation were possible, as in the Drell-Yan case shown in Fig. 6, our boundary η_0 would be a function of mass only.

TABLE III. Physical cross sections in pb and perturbative boundaries at $m = 150$ GeV and $\sqrt{S} = 1.8$ TeV. The corresponding LSvN predictions are also shown.

$\sigma_{q\bar{q}}(m = 150$ GeV; DIS)	$\mu/m = 0.5$	$\mu/m = 1$	$\mu/m = 2$
NLO	9.42	9.31	8.57
$\sigma_{q\bar{q}}^{\text{pert}}$	9.76	9.92	9.31
LSvN($\mu_0 = 0.1m$)	7.9	10.0	9.7
$\eta_0(\mu)$	0.0017	0.0024	0.0028
$\eta(\mu_0 = 0.1m,\mu)$	0.02	0.005	0.00125

$\sigma_{gg}(m = 150$ GeV; $\overline{\text{MS}})$	$\mu/m = 0.5$	$\mu/m = 1$	$\mu/m = 2$
NLO	2.51	2.22	1.81
$\sigma_{gg}^{\text{pert}}$	2.53	2.30	1.89
LSvN($\mu_0 = 0.2m$)	1.76	4.38	-
$\eta_0(\mu)$	0.033	0.055	0.083
$\eta(\mu_0 = 0.2m,\mu)$	0.032	0.004	0.0005

TABLE IV. Physical cross sections in pb for the $q\bar{q}$ channel: DIS versus $\overline{\text{MS}}$ scheme.

m (GeV)	$\sigma_{q\bar{q}}$(DIS; $\overline{\text{MS}}$)	$\mu/m = 0.5$	$\mu/m = 1$	$\mu/m = 2$
100	NLO	52.3; 54.6	52.4; 55.0	48.9; 51.3
	$\sigma_{q\bar{q}}^{\text{pert}}$	53.9; 56.8	55.5; 59.4	52.8; 57.2
125	NLO	21.1; 21.9	21.0; 21.8	19.5; 20.1
	$\sigma_{q\bar{q}}^{\text{pert}}$	21.9; 22.9	22.3; 23.7	21.1; 22.6
150	NLO	9.42; 9.68	9.31; 9.53	8.57; 8.73
	$\sigma_{q\bar{q}}^{\text{pert}}$	9.76; 10.16	9.92; 10.42	9.31; 9.87
175	NLO	4.46; 4.54	4.39; 4.43	4.01; 4.02
	$\sigma_{q\bar{q}}^{\text{pert}}$	4.63; 4.78	4.69; 4.87	4.37; 4.58
200	NLO	2.20; 2.21	2.15; 2.14	1.96; 1.93
	$\sigma_{q\bar{q}}^{\text{pert}}$	2.29; 2.34	2.30; 2.37	2.14; 2.21

We may contrast the modest changes of our $\eta_0(\mu)$ with the fact that the IR boundary of LSvN varies by 3 orders of magnitude in the $\overline{\text{MS}}$ scheme. This large change is partly responsible for the unstable behavior of LSvN's cross section with μ. In the DIS scheme, the IR boundary varies by an order of magnitude for $\mu_0 = 0.1m$ (the value used for their central value prediction in Ref. [4]), and at $\mu/m = 1$ it is twice as large as our η_0. The fact that these quantities are of the same order of magnitude makes LSvN's and our final predictions for the $q\bar{q}$ cross section comparable. Since the $q\bar{q}$ channel is dominant, our final predictions for the total $t\bar{t}$ cross section at the Tevatron are also equal within uncertainties.

Scheme dependence is an extra source of theoretical uncertainty, but it should produce minimal differences for physical cross sections. The results in Tables II and III show that this is not true of the LSvN cross sections. We provide our main predictions in the $\overline{\text{MS}}$ factorization scheme [5]. To check for possible scheme-dependent uncertainty, we perform our resummation for the dominant $q\bar{q}$ channel in both schemes. The cross sections presented in Table IV show that scheme dependence is insignificant in our approach, resulting in a difference of about 4% for the cross section.

In a very recent paper [19] doubts are expressed about the numerical importance of resummation for top-quark production at Fermilab Tevatron energies, and criticisms are leveled at our formalism and that of Ref. [3]. We consider the criticisms unfounded. The analysis presented in our current paper substantiates the work we presented in Ref. [5]. As demonstrated in Sec. III, our perturbative resummation exponent, e.g., Eq. (63), contains no factorially growing terms in its expansion. The analysis we present of our Figs. 1–5 shows that the perturbative region in which we apply resummation remains far removed from the part of phase space in which renormalon poles or nonperturbative residual uncertainty could be influential. Upon expansion in terms of the QCD coupling strength, fixed at the scale of the top-quark mass, our formalism produces the universal leading-logarithmic structures that are found at next-to-leading order (one-loop) in top-quark production and at two loops in the Drell-Yan process. This is an all-orders expansion, but it is convergent because its coefficients do not have factorial growth, and the momentum scale of these structures is restricted to our calculable perturbative regime. Our approach is consistent with,
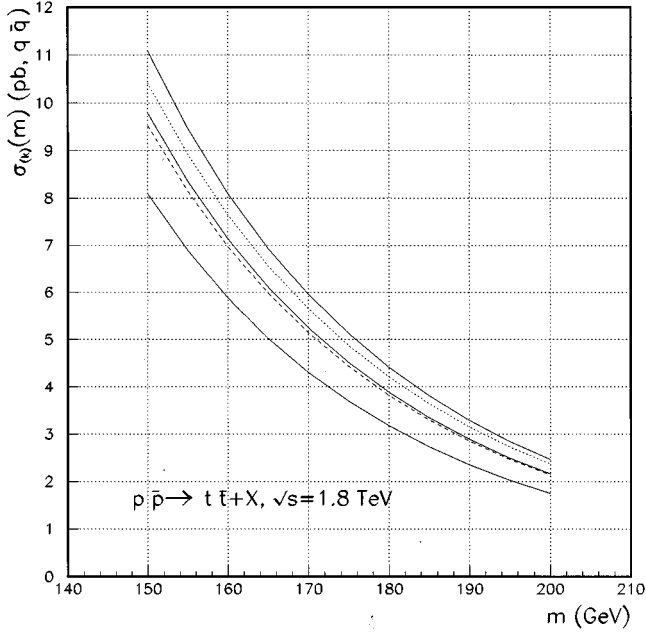
FIG. 10. Physical cross sections in the $q\bar{q}$ channel in the $\overline{\text{MS}}$ scheme. The solid lines denote the finite-order partial sums of the universal leading-logarithmic contributions from the explicit $O(\alpha)$ and $O(\alpha^2)$ calculations for the $t\bar{t}$ and Drell-Yan cross sections, respectively, integrated throughout phase space. Lower solid, $\sigma^{(0)}$; middle solid, $\sigma^{(0+1)}$; upper solid, $\sigma^{(0+1+2)}$. The dashed curve represents the exact next-to-leading-order calculation for $t\bar{t}$ production, in excellent agreement with $\sigma^{(0+1)}$. The dotted curve is our resummed prediction.

and makes maximum use of, the perturbative properties of QCD and established finite-order calculations for the relevant processes. With respect to the numerical importance of resummation, we remark that the enhancement of the cross section produced by resummation in our calculation is a modest 10% above the next-to-leading-order result, at a top mass of 175 GeV and $\sqrt{S}=1.8$ TeV. That the increase cannot be much less than 10% is suggested simply by an examination of the leading-logarithmic contributions at the two-loop level, described in Fig. 10. The suppression of the effects of resummation arises from the retention in Ref. [19] of numerically significant nonuniversal subleading logarithmic terms. As we emphasize in this paper, in a consistent treatment one should retain only the universal logarithmic terms in momentum space and restrict the phase space integration to the region in which the unknown subleading terms would not be significant regardless. We judge that the approach of Ref. [19] is incorrect. As shown first by LSvN [3], it is not necessary to transform to moment space or to resum in order to obtain an increase of the cross section in the neighborhood of 10%.

VI. ESTIMATES OF NON-PERTURBATIVE CONTRIBUTIONS

In this section we hazard some estimates of the nonperturbative contributions. This discussion is based on educated guesses founded mainly on our intuition of what a physical threshold is as well as on the behavior of parton distributions

near the threshold. Since even the gluon parton distributions are not altogether well established, our estimates may be viewed as rough physical understanding expressed quantitatively.

An examination of Fig. 8 indicates that the nonperturbative regime is very small, especially for the $q\bar{q}$ channel. We focus on this channel first, where the support of the nonperturbative interval is $\eta_0\simeq0.008$. We recall that the area under the next-to-leading-order curve is already included in our resummed cross section. Concentrating on the solid curve, we assume that the threshold behavior in the nonperturbative regime is a finite continuation of the solid curve to $\eta=0$. Reasonable guesses include a continuation of the solid curve as a constant from its peak value down to $\eta=0$, or, at most, as a smooth function having the same slope as the solid curve just above the peak. In the former scenario we get an extra contribution

$$\delta\sigma_{q\bar{q}}\simeq5\times0.008=0.04 \text{ pb.} \tag{157}$$

In the latter case we add a further

$$\delta'\sigma_{q\bar{q}}\simeq\frac{1}{2}(15-10)\times0.008=0.02 \text{ pb.} \tag{158}$$

The total is

$$\Delta\sigma_{q\bar{q}}\simeq0.06 \text{ pb.} \tag{159}$$

Since the perturbative cross section at $m=175$ GeV is $\sigma_{q\bar{q}}^{\text{pert}}=4.87$, the extra contribution amounts to an increase of about $1-1.5$ %.

For the gg-channel displayed in Fig. 8(b), $\eta_0\simeq0.05$, and we find

$$\Delta\sigma_{gg}\simeq\frac{1}{2}(2-1)\times0.05=0.025 \text{ pb.} \tag{160}$$

Given that $\sigma_{gg}^{\text{pert}}\simeq0.65$ pb, this correction is a 4% effect. We estimate that the total nonperturbative correction cannot be more than

$$\Delta\sigma^{t\bar{t}}\simeq0.02\sigma_{\text{pert}}^{t\bar{t}}. \tag{161}$$

Correspondingly, we can expect a maximum cross section of about 5.7 pb at $m=175$ GeV.

VII. DISCUSSION AND CONCLUSIONS

There are two main aspects of this paper, one of a more theoretical nature and the other phenomenological. First, we describe in all generality features of *perturbative* resummation that occur in a variety of hard scattering processes while focusing on the specific process of $t\bar{t}$ production. This process has the advantage of being physically very interesting in PQCD in that it probes our understanding of the theory when *multiple* physical scales are involved. It is characterized by an unquestionably large physical scale, m, and a *partonic*

variable η that, in turn, is the ratio of two large scales. It is an ideal process in which one may examine the systematics of partonic interactions in more detail than previously possible. In this process, we encounter difficulties that have challenged the applicability of PQCD for a long time, notably IR renormalons and large color factors, as well as the systematics of universality and invariance under changes of the hard scale. In dealing with $t\bar{t}$ production, we treat all these issues in a *concrete*, phenomenologically significant way.

Second, the paper is concerned with predictions for the total $t\bar{t}$ cross section and the practical application of the theoretical resolutions developed in the first part. At the same time, comparisons are made with next-to-leading-order cross sections and with earlier resummation calculations, and extensive discussions are presented of theoretical limitations and uncertainties.

Our theoretical analysis shows that perturbative resummation without a model for nonperturbative behavior is both *possible* and advantageous. In perturbative resummation, the perturbative region of phase space is separated cleanly from the region of nonperturbative behavior. The former is the region where large threshold corrections exponentiate but behave in a way that is *perturbatively stable*. The asymptotic behavior of the QCD perturbative series, including large multiplicative color factors, is flat, and excursions around the optimum number of perturbative terms does not create numerical instabilities or intolerable RG-dependence. Infrared renormalons are far away from the stability plateau and, even though their presence is essential for defining this plateau, they are of no numerical consequence in the perturbative regime. Large color factors, which are multiplicative, enhance the IR renormalon effects and contribute significantly to limiting the perturbative regime.

As expected in a process with two physical scales, the constraint that ensures good perturbative behavior is a function of several parameters. Making the customary assumption that the renormalization scale is identified with the factorization scale (we denote this single scale by μ), and denoting the variable that probes the partonic threshold by η, we may summarize the essence of our perturbative resummation procedure as follows.

The threshold logarithmic corrections are exponentiated in an exponent

$$E = E(x, \alpha(\mu), m/\mu, N(\mu)), \qquad (162)$$

where $x = \ln[1/(1-z)]$. If the total center-of-mass energy $\sqrt{S}$ is not far above threshold, $\eta \simeq S/4m^2 - 1 \simeq (1-z)/2$. The number of perturbative terms $N(\mu)$ depends on the hard scale only, as long as IR renormalons are far away. The cross section is insensitive to fine-tuning of this number, as long as we remain in a specific well-defined perturbative region of x. In this paper, we determine this region in momentum space by demanding that the cross section conforms to *perturbative* power counting. The cross section is a series multiplying the exponentiated effects of the threshold and whose successive terms are given by functions of the successive derivatives $\partial^k E/k! \partial x^k$. Perturbative power counting means that higher derivatives are suppressed relative to lower ones, because they contribute subleading logarithmic structures in
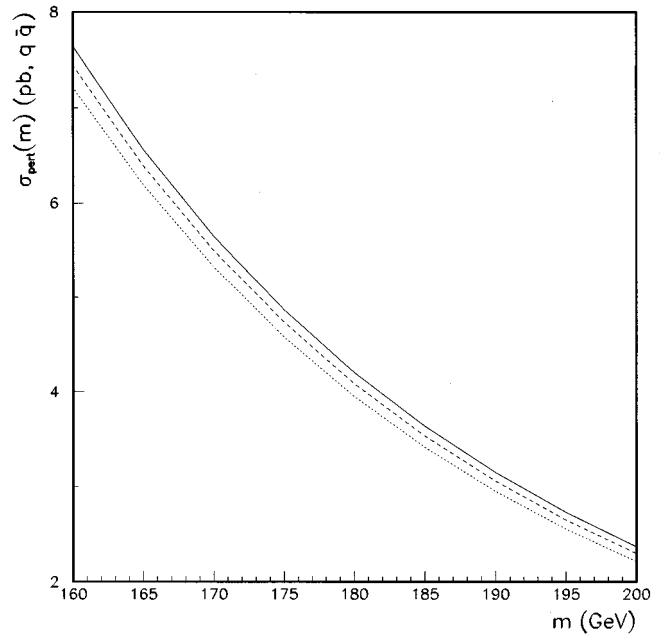

FIG. 11. Physical cross sections for the $q\bar{q}$ channel in the $\overline{\text{MS}}$ scheme: Leading-logarithm resummed cross sections for $\mu/m = 1$ (solid) and $\mu/m = 2$ (dotted) and the Drell-Yan resummed version for $\mu/m = 1$ (dashed).

$\ln[1/(1-z)]$. This statement of perturbative power counting is the essence of perturbation theory. Imposing its validity in the two-scale parameter space, we determine the perturbative regime:

$$\frac{\partial}{\partial x} E(x, \alpha(\mu), m/\mu, N(\mu)) \lesssim 1. \qquad (163)$$

This constraint restricts several sources of nonperturbative behavior, namely: IR renormalons, $\alpha(\mu)$, x, and color factors. Some of them are channel independent while others depend on the nature of the interacting partons. The constraint serves to identify the only unknown in the problem, i.e., the momentum range in x in which perturbative resummation is justified.

We calculate

$$\sigma^{t\bar{t}}(m = 175 \text{ GeV}, \sqrt{s} = 1.8 \text{ TeV}) = 5.52^{+0.07}_{-0.42} \text{ pb}. \qquad (164)$$

Our total $t\bar{t}$-production cross section at $m = 175$ GeV and $\sqrt{S} = 1.8$ TeV is 10 – 14 % greater than that of earlier calculations. Part of the increase comes from the more recent parton distributions we use. Our resummed cross sections are about 9% above the next-to-leading-order cross sections computed with the same parton distributions. The renormalization-factorization scale dependence of our cross section is fairly flat, resulting in a 9 – 10 % theoretical uncertainty. This variation is smaller than the corresponding dependence of the next-to-leading-order cross section, and it is much smaller than the corresponding dependence of the resummed cross section of Ref. [3]. There are other perturbative uncertainties, such as dependence on parton distribu-

tions and factorization scheme. Each of these sources affects our cross section minimally, at level of 4% or less. These variations are not independent, so we opt not to add them in estimating the theoretical uncertainty. For example, different parton distributions are associated with different values of Λ and therefore of α_s. This uncertainty is correlated with uncertainty in α_s from other measurements, *and* with the standard μ variation that we use. Additional back-of-the-envelope modeling of nonperturbative behavior does not increase our cross section more than 2%. However, we do not claim to address the issue of possible nonperturbative enhancements other than at the level of a conservative educated guess.

Our theoretical analysis and the stability of our cross sections under μ variation provide confidence that our perturbative resummation procedure yields an accurate calculation of the inclusive top-quark cross section at Tevatron energies and exhausts present understanding of the perturbative content of the theory. Our prediction agrees with data, within the large experimental uncertainties. We anticipate the greater precision of top-quark production data from future Tevatron collider runs will be instrumental in a fundamental test of

perturbative QCD. The data may also guide the modeling of the nonperturbative phase of the theory and provide a glimpse of phenomena beyond the standard model.

The methodology described in this paper can be applied in several closely related situations. The production of bottom quarks in hadron reactions at energies typical of the Fermilab fixed-target program or the HERA-B facility should be sensitive to the same type of threshold enhancements. Other reactions include the production of hadronic jets with very large values of transverse momentum, the production of pairs of heavy particles predicted in supersymmetry models, or the production of very massive lepton pairs in Tevatron collider experiments. We hope to address these topics in the near future.

[1] P. Nason, S. Dawson, and R.K. Ellis, Nucl. Phys. **B303**, 607 (1988); **B327**, 49 (1989); **B335**, 260(E) (1990).

[2] W. Beenakker, H. Kuijif, W.L. van Neerven, and J. Smith, Phys. Rev. D **40**, 54 (1989); W. Beenakker, W.L. van Neerven, R. Meng, G.A. Schuler, and J. Smith, Nucl. Phys. **B351**, 507 (1991).

[3] E. Laenen, J. Smith, and W.L. van Neerven, Nucl. Phys. **B369**, 543 (1992).

[4] E. Laenen, J. Smith, and W.L. van Neerven, Phys. Lett. B **321**, 254 (1994).

[5] E. Berger and H. Contopanagos, Phys. Lett. B **361**, 115(E) (1995); in Proceedings of the International Symposium on Heavy Flavor and Electroweak Theory, Beijing, China, 1995, Report No. hep-ph/9512212 (unpublished).

[6] G. 't Hooft, in *The Whys of Subnuclear Physics*, Proceedings of the International School, Erice, Italy, 1977, edited by A. Zichichi, Subnuclear Series Vol. 15 (Plenum, New York, 1979); Y. Frishman and A.R. White, Nucl. Phys. **B158**, 221 (1979); in *Large-Order Behavior in Perturbation Theory, Current Physics - Sources and Comments*, edited by J.C. Le Guillou and J. Zinn-Justin (North-Holland, Amsterdam, 1990); G.B. West, Phys. Rev. Lett. **67**, 1388 (1991); L.S. Brown, L.G. Yaffe, and C. Zhai, Phys. Rev. D **46**, 4712 (1992); V.I. Zakharov, Nucl. Phys. **B385**, 452 (1992); M. Beneke and V.I. Zakharov, Phys. Rev. Lett. **69**, 2472 (1992); A.H. Mueller, in *QCD—20 Years Later*, Proceedings of the Workshop, Aachen, Germany, 1992, edited by P.M. Zerwas and H.A. Kastrup

(World Scientific, Singapore, 1993).

[7] H. Contopanagos and G. Sterman, Nucl. Phys. **B419**, 77 (1994); B.R. Webber, Phys. Lett. B **339** 148 (1994); A.V. Manohar and M.B. Wise, *ibid.* **344**, 407 (1995); G.P. Korchemsky and G. Sterman, Nucl. Phys. **B437**, 415 (1995).

[8] M. Beneke and V.M. Braun, Nucl. Phys. **B454** 253 (1995).

[9] H. Contopanagos (in preparation).

[10] H. Contopanagos and G. Sterman, Nucl. Phys. **B419**, 77 (1994).

[11] H. Contopanagos and G. Sterman, Nucl. Phys. **B400**, 211 (1993).

[12] L. Alvero and H. Contopanagos, Nucl. Phys. **B436**, 184 (1995); **B456**, 497 (1995).

[13] G. Sterman, Nucl. Phys. **B281**, 310 (1987); S. Catani and L. Trentadue, *ibid.* **B327**, 323 (1989); **B353**, 183 (1991).

[14] H. Contopanagos, E. Laenen, and G. Sterman, Report No. hep-ph/9604313 (unpublished).

[15] H. L. Lai *et al.*, Phys. Rev. D **51**, 4763 (1995).

[16] R. Hamberg, W.L. van Neerven, and T. Matsuura, Nucl. Phys. **B359**, 343 (1991).

[17] CDF Collaboration, P. Azzi, in *QCD and High Energy Hadron Interactions*, Proceedings of the XXXI Recontres de Moriond, Les Arcs, France, 1996 (unpublished); DO Collaboration, P. Bhat, *ibid.*

[18] J. Collins and R.K. Ellis, Nucl. Phys. **B360**, 3 (1991).

[19] S. Catani, M. Mangano, P. Nason, and L. Trentadue, CERN Report No. CERN-TH/96-21, hep-ph/9602208 (unpublished).